Materials Advances

ROYAL SOCIETY OF CHEMISTRY

REVIEW

View Article Online
View Journal

Cite this: DOI: 10.1039/d6ma00008h

Metallenes: synthesis, properties, and applications in electrocatalysis and energy storage

E. S. Sowbakkiyavathi,†[ab] Aakash Carthick Radjendirane,†[ac] Ju Hyun Oh,[c] Seung Jun Lee*[c] and Subramania Angaiah *[ac]

Metallenes, a newly emerging class of atomically thin metallic nanosheets, have attracted significant interest because of their abundance of catalytically active sites, tunable electronic structure, and distinctive two-dimensional shape. Advanced synthetic strategies, including liquid-phase exfoliation, template-assisted growth, and chemical reduction, enable precise control over thickness, composition, and surface chemistry, leading to physicochemical properties that surpass those of their bulk counterparts. Owing to their remarkable mechanical flexibility, electrical conductivity, and surface reactivity, metallenes have demonstrated remarkable performance in electrochemical applications. Notably, they exhibit enhanced catalytic activity and stability for CO_2 reduction, oxygen reduction, and hydrogen evolution reactions, achieving lower overpotentials and improved durability. In energy storage systems, metallenes facilitate rapid ion transport and high charge storage capacity, thereby improving the efficiency of supercapacitors and rechargeable batteries when used as active electrodes or conductive frameworks. This review critically summarizes recent advances in synthesis methodologies, structure–property relationships, and catalytic mechanisms, while outlining key challenges related to scalable production, long-term stability, and device integration. Future research directions focusing on the rational structural design of multifunctional hybrid systems are proposed to accelerate their practical deployment in next-generation energy technologies.

Received 3rd January 2026,
Accepted 9th March 2026

DOI: 10.1039/d6ma00008h

rsc.li/materials-advances

1. Introduction

Two-dimensional (2D) materials have had a profound impact on nanoscience and technology since the discovery of graphene. In general, graphene is a 2D ultrathin sheet composed of sp^2-hybridized carbon atoms arranged in a honeycomb lattice, which results in exceptional mechanical behaviour and excellent thermal and chemical stability.[1,2] Following the

[a] Electro-Materials Research Laboratory, Centre for Nanoscience and Technology, Pondicherry University, Puducherry – 605 014, India. E-mail: a.subramania@gmail.com
[b] Department of Physics, Sathyabama Institute of Science and Technology, Chennai – 600 119, India
[c] Department of IT-Energy Convergence (BK21 FOUR), Korea National University of Transportation, Chungju-27469, Republic of Korea. E-mail: sjlee@ut.ac.kr
† These authors contributed equally.

E. S. Sowbakkiyavathi

Sowbakkiyavathi E. S. is an Assistant Professor at the Department of Physics, Sathyabama Institute of Science and Technology, Chennai, India. She did her PhD research at Pondicherry University, India. Her current research interests include the development of nanostructured materials for M-ion batteries, supercapacitors, DSSCs, and electrocatalysis for water splitting.

Aakash Carthick Radjendirane

Aakash Carthick Radjendirane is a PhD student at the Centre for Nanoscience and Technology, Pondicherry University, Puducherry, India, under the supervision of Prof. Subramania Angaiah. He received his MTech in Nanoscience and Technology from Pondicherry University in 2020. His current research focuses on the development of solid electrolytes as well as hydrogel electrolytes for metal-ion batteries.

discovery of graphene, several 2D materials similar to graphene have been developed, including transition-metal dichalcogenides (such as MoS_2 and WS_2), MXenes, black phosphorus, and boron nitride. Furthermore, the combination of electrical, chemical, and structural behaviour has enabled 2D materials to be used in a wide range of applications, particularly in electrocatalysis and energy storage devices.[3–5]

Despite rapid advancements in 2D materials, an important impediment remains: developing metallic 2D materials that can retain the metal's characteristic properties, such as electron density and metallic bonding, while maintaining exceptional electrical and thermal behaviour, without compromising the structural and quantum confinement of 2D materials. On the other hand, bulk metals have limitations in terms of surface area and adaptability, despite being chemically versatile and naturally conductive. Hence, materials that combine the advantages of bulk metals with 2D nanostructures will be promising candidates for next-generation technologies.[6,7]

To combat these challenges, metallenes, which are a newer class of atomically thin metallic nanosheets, have been developed. Generally, metallenes are metallic sheets with a single or a few layers, where the structural framework is dominated by the metallic bonding. The metallenes are composed of ultrathin metal sheets, only a few atomic layers thick, exhibiting excellent electrical, thermal, and chemical properties that are absent in their bulk counterparts. Unlike conventional metals, metallenes have an exposed surface with a high density of undercoordinated atoms, resulting in excellent features of enhanced catalytic activity, high surface reactivity, and tunable optical responses.[8,9] Furthermore, metallenes with reduced dimensionality are highly favourable for quantum confinement effects, altering the electronic density of states and resulting in changes in conductivity, magnetism, and chemical stability compared to their bulk counterparts.

In comparison with conventional metals and other 2D materials, metallenes offer unique advantages of combined electrical, mechanical, thermal, and chemical stability, which are highly beneficial for electrocatalysis and energy storage device applications.[10,11] The metallenes, with an abundance of delocalized electrons within the ultrathin metallic lattice, are crucial for rapid electron transfer. Furthermore, metallenes have substantially higher catalytic behaviour than bulk metals. The large number of under-coordinated surface atoms, coupled with size-dependent quantum effects, provides a plethora of active sites that are effectively involved in various electrocatalysis processes, such as the hydrogen evolution reaction (HER), oxygen evolution reaction (OER), CO_2 reduction, and nitrogen fixation. Metallenes encompass monometallic thin sheets, such as Ni, Co, Fe, Cu, Pt, Ru, and Rh; bimetallic nanosheets, such as CoNi, NiFe, and PtRu; and complex high-entropy metallenes that combine multiple metal elements in a single ultrathin structural framework. Similarly, in energy storage device applications, various materials, such as antimonene, germanene,

Ju Hyun Oh

Ju Hyun Oh earned his PhD in Organic Chemistry from Gyeongsang National University in 2023. From 2019 to 2020, he gained broad research experience as a visiting student in Sessler's group at The University of Texas, Austin, as well as a senior researcher at Gyeongsang National University. He is currently a researcher in the Department of IT- Energy Convergence at the Korea National University of Transportation. His current research focuses on the synthesis of organic ligands for surface-functionalized MXenes and on the development of high-performance composite materials for energy applications.

Seung Jun Lee

Seung Jun Lee is a professor in the Department of IT - Energy Convergence at the Korea National University of Transportation. He earned his PhD in Physical Chemistry from Gyeongsang National University and he also gained broad research experience as a senior researcher at the Photochemical & Nanomaterials Core-Facility Center at Gyeongsang National University. He is currently conducting active research primarily on two-dimensional (2D) materials and metal-ion batteries. His current research focuses on the development of high-performance composite materials for energy applications.

Subramania Angaiah

Subramania Angaiah is a Professor at the Centre for Nanoscience and Technology, Pondicherry University, India and a visiting Professor of Jiangsu University of Science and Technology (JUST), Zhenjiang 212003, China. He did his post-doctoral research at KIST, South Korea. His current research focuses on the development of nanostructured materials for M-ion batteries and supercapacitors; solid electrolytes/hydrogel electrolytes for metal-ion batteries; functional materials for DSSCs, QDSSCs, and PSCs; electro-catalysis for water splitting, secondary metal recovery from waste and bio-sensors and bio-imaging.

and stanene, have been utilised to form high-performance electrodes due to their ultra-thin metal nature, enabling rapid charge transfer.[12–14] Furthermore, the high surface-to-volume ratio maximizes their interaction with surrounding molecules, thereby enhancing their performance in chemical, electrochemical, and biological applications.[15]

Most importantly, metallenes serve as a conceptual and functional bridge between conventional 2D materials and bulk metals. In the case of graphene and MXenes, which have a large surface area and tunable electrical behaviour, their metallic nature is limited in particular phases. In contrast, bulk metals exhibit high conductivity but often fail in structural refinements and surface exposure required for catalytic and energy-related applications.[16–18] Regarding metallenes, they merge the features of both groups, combining intrinsic metallic characteristics with the benefits of a 2D structure, making them an excellent candidate for next-generation technologies such as electrocatalysis, energy storage, and conversion devices.[19]

Hence, the present review primarily focuses on gaining insight into metallenes, beginning with their classifications and the structural diversity that distinguishes them from other 2D materials. It also deliberates various synthesis methodologies, ranging from top-down exfoliation strategies to bottom-up chemical growth approaches, which are also critically addressed. Furthermore, it also extensively investigated the development of metallenes for electrocatalysis and energy storage applications. Finally, the current challenges associated with metallenes from all perspectives are critically reviewed, along with potential optimization strategies and future research directions aimed at advancing their applications in next-generation energy technologies.

2. Structure and classification of metallenes

In 2018, the term ''metallene'' was coined to describe the two-dimensional topography of metals.[20] A single or a few atomic sheets of metal atoms organized in a highly ordered planar or slightly bowed lattice make up metallenes, which are atomically thin, two-dimensional (2D) metallic layers, as shown in Fig. 1. Metallenes have much lower coordination than their bulk metallic equivalents, which have high coordination numbers and isotropic bonding. This leads to a high percentage of surface-exposed and unsaturated metal atoms. Significant modifications in electronic structure, such as altered charge distribution, improved surface electron density, and modified d-band states, are brought about by this particular atomic arrangement. Depending on the element and synthesis technique, the lattice of metallenes may take on hexagonal, trigonal, or mixed coordination geometries; interatomic distances are frequently widened as a result of decreased dimensional confinement and surface strain. Altogether, these structural characteristics offer a remarkably high surface-to-volume ratio, a large number of accessible active sites, and robust metal-electrolyte interactions, all of which support their outstanding

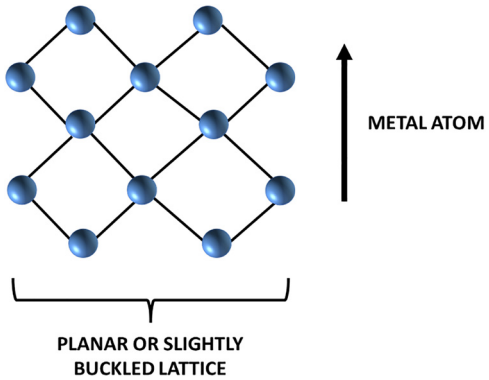

Fig. 1 Conceptual illustration of an atomically thin metallene with a two-dimensional atomic arrangement.

catalytic and electrochemical performance. The chemical reactivity of metallenes is further enhanced by the presence of intrinsic defects, edge sites, and potential lattice distortions, which make their structure extremely adaptable for specific use in electrocatalysis and energy storage.

The structure of metallenes can be classified into two primary categories – layered and non-layered metals – due to the variations in metal characteristics.[21] The schematic classification of two-dimensional materials from X-enes to metallenes and an overview of the metallene family based on elemental composition and publication trends of metallenes over the past 10 years are shown in Fig. 2(a–c). The structure of metallenes significantly impacts their preparation methods. The structure of layered metal compounds, such as bismuthene and antimonene, resembles that of phosphorus, which has a six-membered atomic structure resembling a rhombus.[22] Physical anisotropy results from variations in the in-plane and out-of-plane atomic distances.[23] Top-down exfoliation techniques, including mechanical and ultrasonic exfoliation, can successfully produce antimonene and bismuthene based on their structural characteristics. But other metals, such as magnesium, have substantial isotropy and are not stacked. It is challenging to reduce the vertical dimension of non-layered metal materials while maintaining other dimensions constant because of their intrinsic isotropic chemical bonding capabilities. Unlike layered materials, they show flexible deformation under external mechanical forces and a three-dimensional structure at the microscopic level instead of a two-dimensional crystal structure. As a result, creating non-layered metal-based metallenes *via* a straightforward top-down approach is challenging.[24] However, by altering the reaction circumstances, these obstacles might be removed. For example, Zhang *et al.* described a method for physically exfoliating non-layered metallic magnesium crystals into their 2D structural counterparts using low temperatures.[25]

Antimonene and other layered metallenes have distinct atomic arrangements. The characteristics of nanosheets will be affected by folding structures with various transport orientations, and the conformation of various allotropes is shown in Fig. 3a. With four atoms in the unit cell, arranged in a

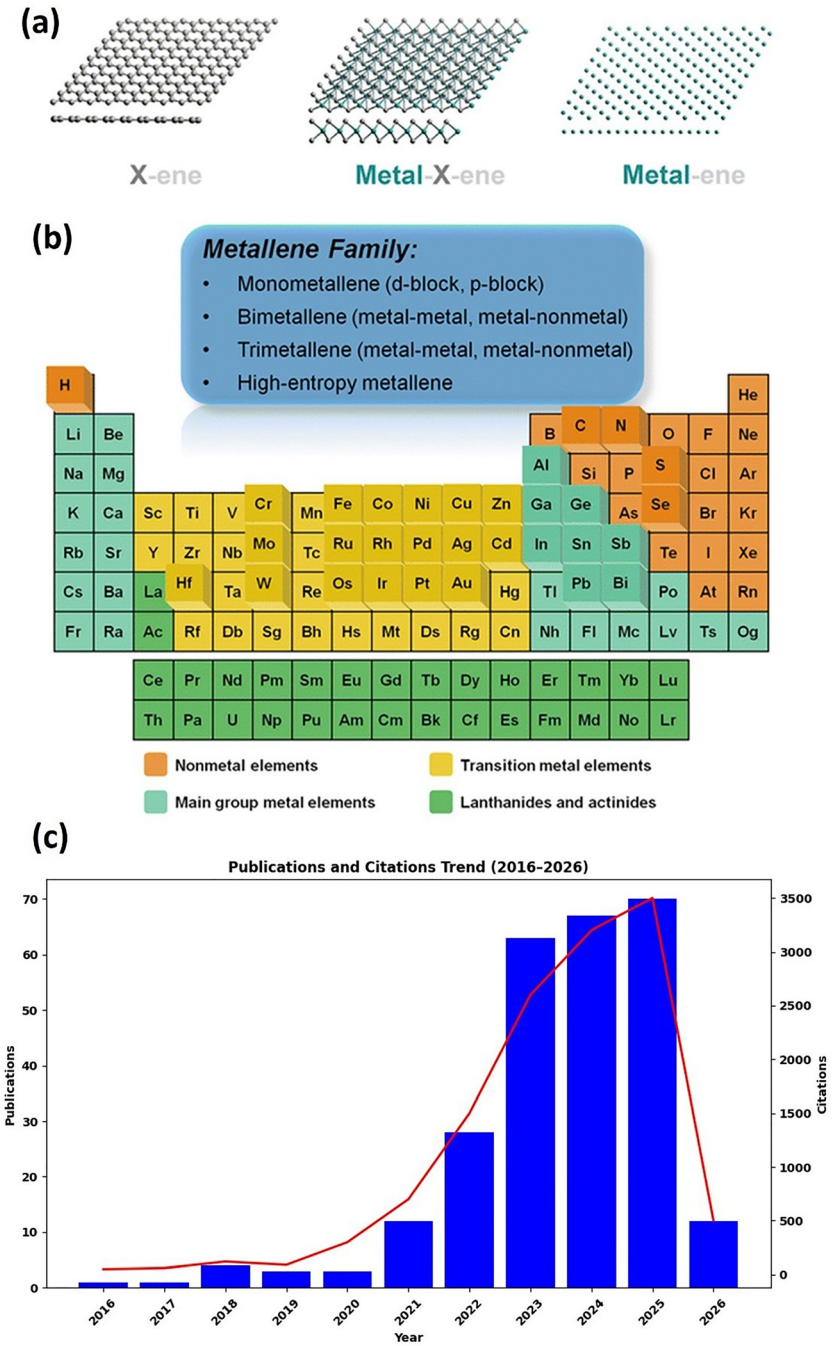

Fig. 2 (a) Schematic comparison of X-ene, metal-X-ene, and metal-ene structures, (b) classification of the metallene family (mono-, bi-, tri-, and high-entropy metallenes) with representative elemental distribution across the periodic table, (c) publication and citation trends of metallene research from 2016 to 2026 (data from the Web of Science).

rectangular lattice, and two non-coplanar sublayers, α-Sb has a twisted atomic structure that results in a wrinkled surface. Sb and Sb have bond lengths of 2.83 and 2.91 Å, respectively, and bond angles of 95.0° and 102.51°, respectively. The bond angle of the hexagonal lattice β-Sb is 89.91°. The most stable structure is buckled β-Sb, whereas puckered α-Sb is the lower-energy shape.[26] Furthermore, the structures of bismuthene are comparable. The structure of the buckling β-Bi resembles a honeycomb and has a 2D hexagonal lattice (Fig. 3b).[27] Bismuthene α-Bi's washboard structure is made up of two atomic layers in a single layer. Because of their strong in-plane bond and isotropic characteristics, non-layered metallenes typically form extremely densely packed crystal structures (Fig. 3c–h). For instance, two triangular sublattices make up the germanene honeycomb lattice (Fig. 3c).[28] Germanene exhibits a buckled structure when viewed from the side. Stanene is typically made of a low-buckled

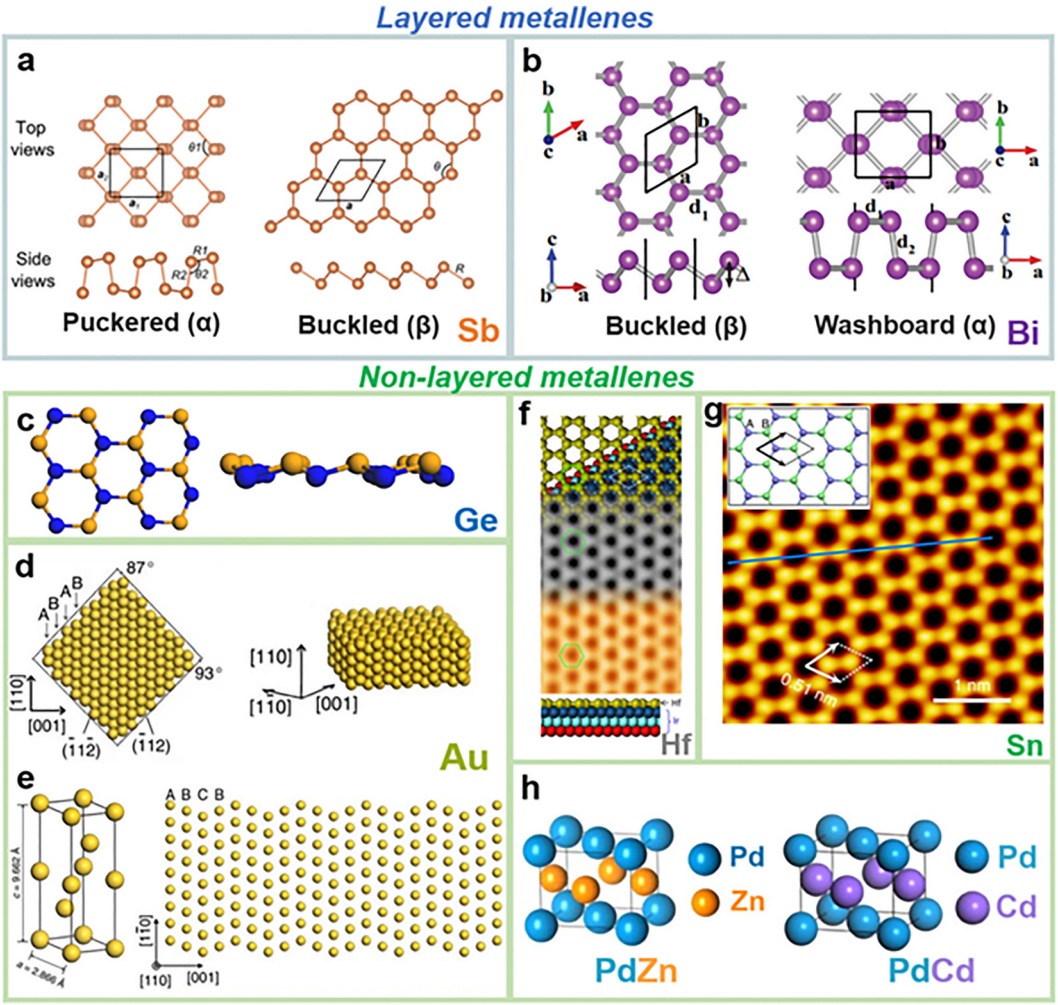

Fig. 3 Atomic configurations of layered and non-layered metallenes. (a) Atomic configurations of antimonene allotropes, (b) atomic configurations of bismuthene allotropes, (c) atomic configurations of germanene, (d) crystal structure of a typical AuSS with its basal plane along the $[110]_h$ zone axis, showing ABAB stacking along the $[001]_h$ direction, (e) schematic illustration of a unit cell and crystallographic models of 4H Au, (f) atomic configuration of a Hf honeycomb lattice on Ir(111), (g) high-resolution STM image of the stanene film, inset: schematic atomic model of the honeycomb stanene. (h) Crystal structures of PdZn NSs and PdCd NSs. Reproduced from ref. 15 with permission from the Royal Society of Chemistry.

honeycomb lattice with an atomic layer of tin. However, the findings of anomalous ultra-flat stanene revealed by Deng *et al.* open up new avenues for the study of two-dimensional topological physical materials (Fig. 3g).[29] Furthermore, the architectures of metallenes based on transition metals were investigated. Gold square sheets (Au SSs) with a densely packed hexagonal structure were created *in situ* on graphene oxide by Huang *et al.*[30] The 2D and 3D crystal models of Au SSs show that each nanosheet has a square surface stacked along the $[001]_h$ direction and perpendicular to the $[110]_h$ direction. Along the direction of tight stacking [001]4H, Au nanosheets feature a "ABCB" stacking sequence in addition to the "AB" stacking pattern.[31] Newly reduced Au atoms were deposited on the original Au nanosheets in the three orientations of $[1\bar{1}0]_h$, $[001]_h$, and $[110]_h$, resulting in this distinctive stacking arrangement (Fig. 3e).[32] Moreover, a flat, two-dimensional honeycomb arrangement is seen in the transition metal hafnium. On Ir(111) substrates, Li *et al.* created continuous monolayer Hf films with a fcc/hcp hybrid honeycomb atomic structure.[33] The crystal structure of some alloy nanosheets, such as PdZn and PdCd, is face-centered tetragonal (fct). Pd and M (Zn and Cd) atoms are arranged in a structured manner in this atypical fct phase structure (Fig. 3f). Eight vertices and the centers of the cell's top and bottom faces are occupied by Pd atoms in this arrangement, whereas M atoms occupy the remaining four face centers (Fig. 3h).

3. Properties of metallenes

A new class of two-dimensional materials, called metallenes, arise when the dimensionality of metallic materials is reduced to the atomic scale, specifically to a monolayer or a few atomic layers. In contrast to their bulk counterparts, these atomically thin metallic nanosheets exhibit a range of unique physicochemical properties. Quantum confinement effects, higher

surface-to-volume ratios, and the high density of low-coordination surface atoms inherent in ultrathin structures are the main causes of this shift from bulk behavior.

3.1. Catalytic properties

The large number of coordination-deficient metal atoms in metallenes is one of their most remarkable characteristics. The majority of atoms in bulk metals are completely coordinated by their neighbors and embedded in a periodic lattice. The decreased thickness in metallenes, on the other hand, results in a higher percentage of atoms being exposed at the surface with fewer nearby atoms. Metallenes' activities and selectivity are increased by their enhanced contact with reaction intermediates due to their customizable electronic structure. In addition to improving atomic consumption efficiencies, metallenes' high density of exposed metal atoms makes functionalization with ligands possible. The ultrathin structure, diffusion distance, and charge transfer of reactants are primarily responsible for metallenes' reported high activity, selectivity, and stability in heterogeneous catalytic processes like organocatalysis, electrocatalysis, and photocatalysis. Compared to gold nanoparticles, ultrathin gold nanosheets in organocatalysis show better selectivity for C–H bonding and solvent-free oxidation.[34] Metallenes are very appealing as catalysts because their undercoordinated sites frequently function as extremely active sites for chemical reactions. These unsaturated sites, for instance, can decrease the activation energy for critical phases in catalytic processes, including the carbon dioxide reduction reaction (Co_2RR), oxygen evolution reaction (OER), and hydrogen evolution reaction (HER). For instance, in studies including active cycling, monolayer Pt NSs demonstrate outstanding ORR activity and sustained stability.[35] To efficiently increase the photocatalytic effect, metallenes can be employed as co-catalysts or in conjunction with semiconductor photocatalysis.[36] Furthermore, metallenes' exposed active sites and fascinating catalytic qualities were advantageous in biomedicine. Hexagon bismuth nanosheets were created by Torres *et al.* and can serve as highly conductive electrocatalytic platforms to enhance the charge transfer process. Their superior electrical characteristics enable their application as an adenine dinucleotide (NADH) sensor.[37] Additionally, an antimonene-based phenol biosensor demonstrated superior analytical performance in terms of linearity, sensitivity, selectivity, and reproductivity when contrasted with other Group VA elements.[38] Notably, multi-element metallenes may have superior catalytic qualities over monometallenes because of the varying compositions of the distinct metallenes.[39]

3.2. Magnetic properties

One of the most fascinating features of metallenes' physicochemical behavior is their magnetic properties, especially as these characteristics can differ greatly from those of their bulk counterparts. Collective interactions between localized or itinerant electrons in bulk metals produce magnetism; these interactions usually require particular electronic configurations, such as unpaired d- or f-electrons. However, because of quantum confinement, surface effects, and broken symmetry, the electrical structure can be drastically changed when metallic materials are thinned down to the atomic scale to create metallenes. These modifications frequently result in the amplification or appearance of magnetic ordering that is not present in the bulk phase. For example, even at room temperature, 2D metallenes made of transition metals, including Fe, Co, and Ni, have shown ferromagnetic or antiferromagnetic behavior due to reduced coordination of surface atoms and enhanced spin polarization. Also, spin–orbit coupling and lattice symmetry breakdown can cause metallenes to exhibit magnetic anisotropy, in which the direction of magnetization becomes energetically preferred. While edge states can greatly influence overall magnetic behavior, metallenes' huge surface area and minimal coordination environment improve magnetic moment localization. Because of these characteristics, metallenes hold great promise for use in magnetic sensing technologies, spintronics, and magneto-optical systems. Furthermore, doping, strain engineering, or heterostructure formation can be used to precisely alter spin states and magnetic interactions at the nanoscale, hence tuning the magnetic sensitivity of metallenes. All things considered, research on magnetism in metallenes advances our fundamental understanding of low-dimensional magnetism and opens up new avenues for the development of 2D magnetic materials for next-generation quantum and spintronic devices. Leng *et al.* created several Ni nanosheets with superparamagnetism that varies with size.[40] The magnetism of small Ni nanosheets is weaker than that of big edge-length nanosheets. However, when their size reduces, their coercive force will grow, enhancing Ni nanosheets' anisotropic magnetic characteristics. Meanwhile, Zhao *et al.* discovered that 2D iron nanosheets showed significant perpendicular magnetic anisotropy after using electron beam irradiation to extend a single atomic layer of iron in the porous graphene's perforations.[41] Future research is required to identify additional metallenes with fascinating magnetic characteristics.

3.3. Plasmonic properties

Furthermore, metallenes have fascinating optical and plasmonic characteristics. Metallenes can sustain localized surface plasmon resonances (LSPR), in which conduction electrons collectively vibrate in response to input electromagnetic radiation, because of their metallic conductivity and free electron density.[42] Applications in biosensing, photothermal treatment, and surface-enhanced Raman scattering (SERS) are made possible by these plasmonic modes' remarkable sensitivity to the thickness, shape, and local environment of nanosheets. Metallenes made of a broader range of transition metals, like Pd, Pt, and Cu, can exhibit broad and tunable plasmonic responses due to quantum size effects, altered electronic band structures, and increased surface-to-volume ratios. This is in contrast to bulk metals, where plasmonic behavior is frequently dominated by interband transitions and limited to specific noble metals like Ag and Au, respectively. According to a recent study, the optical absorption energy decreases with increasing 2D Ga and with increasing thickness.[43] The presence of covalent connections between metal layers and the SiC substrate

reduces the quantum confinement effect, which is the source of thickness-dependent resonance energies, when compared to an infinite square well potential. Metallenes' atomic scale thickness results in substantial electromagnetic field augmentation at the nanosheet surface and edges due to improved light–matter interaction, anisotropic charge distribution, and plasmonic field confinement inside the 2D plane. Metallenes are great options for plasmon-enhanced photocatalysis, surface-enhanced Raman scattering (SERS), and nanoscale optical sensors because of their improved near-field effects. Furthermore, by adjusting variables like sheet thickness, lateral dimensions, edge states, doping level, and the surrounding dielectric environment, metallenes' plasmonic resonance can be precisely adjusted. Metallenes are positioned as attractive materials for next-generation plasmonic and photonic devices, especially in the visible and near-infrared (NIR) ranges, due to their tunability and compatibility with flexible and transparent substrates. Huang *et al.* reported a free-standing form of ultrathin hexagonal palladium nanosheets with a size of 20–160 nm and a thickness of less than 10 atomic layers.[44] These nanosheets demonstrated strong SPR (surface plasmon resonance) absorption and significant tunable NIR (near infrared) absorption, which is characteristic of many 2D metal nanostructures with LSPR absorption in the visible (vis) and NIR regions.

Furthermore, metallenes are frequently used in disease research due to their superior optical and photothermal conversion properties.[45] The photothermal performance of multi-element metals may be superior to that of monometallenes in biological applications. For example, compared to pure Au or Pd nanostructures, AuPd nanosheets demonstrated noticeably superior photothermal performance.[46] Additionally, due to their great penetrability, metals' optical absorbance can be extended to the second near-infrared (NIR II, 1000–1700 nm) range, which is ideal for PTT.[47] PtAg NSs had photothermal conversion efficiencies of 19.2% and 45.7% at 785 nm and 1064 nm, respectively, with wide absorption from 400 to 1200 nm.[48] For biological applications, including PTT, biosensors, and bioimaging, the plasmonic qualities of metallenes are quite alluring.

3.4. Photoluminescence properties

The study of two-dimensional (2D) metallic systems is gaining interest in the photoluminescence (PL) characteristics of metallenes. This is mainly because bulk metals usually do not show luminescence activity. After all, excited electrons relax quickly without radiating. Metals' electronic band structures, however, are drastically changed when they are reduced to atomically thin sheets, or metallenes. This is frequently the result of quantum confinement, surface atom reconstruction, and decreased dielectric screening. Discrete energy states may arise as a result of these modifications, and excited carriers may recombine radiatively to produce visible PL There have been reports of weak but adjustable PL emissions in certain metallenes, such as atomically thin Au, Pt, or Pd nanosheets; these emissions are frequently in the visible to near-infrared spectrum. Plasmon-enhanced fluorescence mechanisms, localized defect states, or interband transitions may be the source of this emission. Crucially, the wavelength and PL intensity in metallenes are extremely sensitive to external stimuli like strain or electric fields, as well as to surface functionalization, edge shape, and layer thickness. Furthermore, surface imperfections and atomic vacancies can be crucial in modifying PL behavior because of the strong confinement and large surface area of metallenes, offering a practical handle for nanoscale light emission engineering. Because of these characteristics, metallenes are promising candidates for use in light-emitting devices, biosensing, bioimaging, and optoelectronics. Future developments in synthesis, surface passivation, and heterostructure formation are anticipated to improve metallenes' optical efficiency and expand their use in photonic technologies, even though their PL quantum yields are typically lower than those of semiconducting 2D materials like MoS and WS_2, respectively.

According to Hussain *et al.*, the ultrathin Bi nanosheets showed high PL in the visible spectrum.[49] They also discovered that process-related crystal defects and carrier confinement effects may have caused the shift in the PL signal. Under illumination at 470 nm, Zhang *et al.* experimentally confirmed that antimonene produced green fluorescence and had an indirect band gap of roughly 2.33 eV and a PL lifetime of 4.3 ns. Metallenes can be employed in biomedicine as fluorescent biosensors, according to PL characteristics.[50] Liu and colleagues synthesized antimonene quantum dots with superior PL characteristics based on this.[51] When excited at 350 nm, they produced blue fluorescence free from environmental interference, and they can be employed as a pH-mediated dual-channel radiometric fluorescent probe for the detection of tetracyclines. Certain metallenes also show fluorescence quenching, which makes them potentially valuable as biosensors for nucleic acids (DNA, miRNA, *etc.*).[52] Charge transfer between metallenes and dye molecules, as well as fluorescence resonance energy transfer (FRET), is primarily responsible for the exceptional quenching effect of metallenes.[53,54] For instance, palladium and bismuth nanosheets have been employed as nucleic acid detection sensors for miRNA and DNA detection.[55,56]

Collectively, metallenes are a very adaptable and multipurpose class of 2D materials due to their distinctive combination of catalytic, magnetic, plasmonic, and photoluminescence capabilities. While their behavior presents intriguing opportunities for the creation of cutting-edge technologies in energy conversion, electronics, sensing, and information storage, it also challenges conventional notions of metal physics and chemistry. A better comprehension of the structure–property interactions in metallenes will be crucial as this field of study develops to realize their potential in both basic science and real-world applications.

Comparison of metallenes with MXenes. Despite being members of an identical broad class of two-dimensional materials, metallenes and MXenes are very different in terms of composition, surface chemistry, electronic structure, and functional performance, as given in Table 1. Comparison of

Table 1 Comparison between metallenes and MXenes in their structural, electronic, and physicochemical properties

Feature	Metallenes	MXenes
Composition	Pure metal atoms	$M_{n+1}X_nT_x$
Conductivity	Very high metallic	High (surface-dependent)
Thickness	A few atomic layers	A few atomic layers
Surface chemistry	Highly active and modifiable	Surface terminations (–OH, –F, and –O)
Catalytic sites	Abundant, exposed	Moderate
Stability	Can oxidize/aggregate	Depends on the environment
Applications	Electrocatalysis, electrometallurgy (EM), energy storage	Energy storage, electromagnetic interference (EMI) shielding, and catalysis

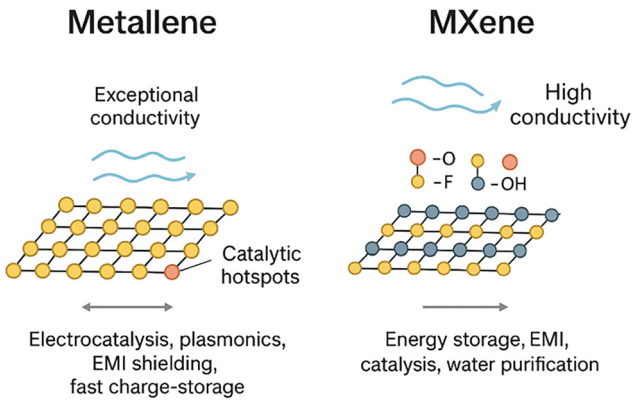

Fig. 4 Schematic comparison of metallenes and MXenes, highlighting differences in surface chemistry, conductivity, and representative application areas.

metallenes and MXenes, highlighting differences in surface chemistry, conductivity, and representative application areas, is schematically given in Fig. 4. Metallenes, which are typically created by exfoliation, template-guided growth, electrochemical stripping, or bottom-up synthesis, are made entirely of pure metal atoms organized in atomically thin layers. These sheets have ultrahigh electron mobility and continuous metallic bonding. On the other hand, MXenes have a more complicated multicomponent formula ($M_{n+1}X_nT_x$) with early transition metals (M), carbon and/or nitrogen (X), and surface terminations (T_x = –O, –OH, –F) added during etching, resulting in a mixture of metallic cores and chemically active surfaces. Even though they are both few-layer systems, MXenes offer structurally defined but termination-dependent sites where the type, density, and arrangement of surface functional groups greatly affect the catalytic activity, while metallenes expose fully metallic, coordinatively unsaturated atoms that function as dense catalytic hotspots. Metallenes have an exceptionally high intrinsic conductivity because of a fully delocalized electron cloud, which makes them perfect for quick charge transfer. In contrast, MXene conductivity varies depending on the termination chemistry, with oxygen-terminated MXenes acting more metallic and fluorine- or hydroxyl-terminated ones exhibiting less electrical transport. Another significant difference is stability: MXenes exhibit environment-dependent oxidation, especially in humid or oxygenated atmospheres, while metallenes may show surface oxidation, aggregation, or reconstruction under ambient conditions due to their high surface energy. Stability improves under inert storage or with surface modification. Because of their superior conductivity and abundance of active sites, metallenes excel in electrocatalysis (HER, OER, and ORR), plasmonics, electromagnetic shielding, and high-rate energy storage. Conversely, MXenes are particularly effective in supercapacitors, Li/Na-ion batteries, EMI shielding, heterogeneous catalysis, water purification, and sensing technologies because of their hydrophilicity, tunable surface terminations, and layered ion-accessible architecture.[57]

4. Synthesis approaches

Metallene nanosheet synthesis techniques can be categorized into top-down and bottom-up methods, just like other 2D materials, as shown in Fig. 5.[58] Using mechanical forces and molecular intercalation to break interlayer bonding, top-down synthesis, which includes mechanical cleavage, ultrasonic exfoliation, electrochemical exfoliation, and plasma-assisted procedures, exfoliates a bulk or powdered sample into nanosheets.[59] In-plane addition or atom or molecule self-assembly chemically facilitates bottom-up synthesis, which includes molecular beam epitaxial, chemical vapor deposition (CVD), and wet chemical synthesis. With their distinctive strong in-plane covalent link frameworks and weak interlayer van der Waals interactions, graphene and TMDs are easily separated into one or a small number of layers through straightforward chemical and mechanical exfoliation.[60,61] On the other hand, a lot of metallenes have a strong propensity to form 3D crystals with good structural symmetry and undergo nondirectional metal bonding. They prefer to form densely packed crystal structures, which makes their nanostructures with a high percentage of unsaturated surface atoms unstable. Consequently, only a small number of metallenes can be produced using the simple top-down synthesis process, and it is challenging to directly separate the bulk intermetallic layers from one another.[62] On the other hand, atomically thin metallenes can be made by adjusting them to promote anisotropic growth kinetics or by adding surfactants, ligands, and templates to help lower the surface bond energy. However, a different approach to metallenes synthesis is a bottom-up chemical synthesis strategy. Temperature-controlled or initiator-assisted precursor breakdown is the first step in the metallene synthesis pathway. This is followed by reduction events that create metal nuclei. The nucleus is therefore able to develop a lateral plane by the interaction of surfactants, ligands, or templates. It is possible

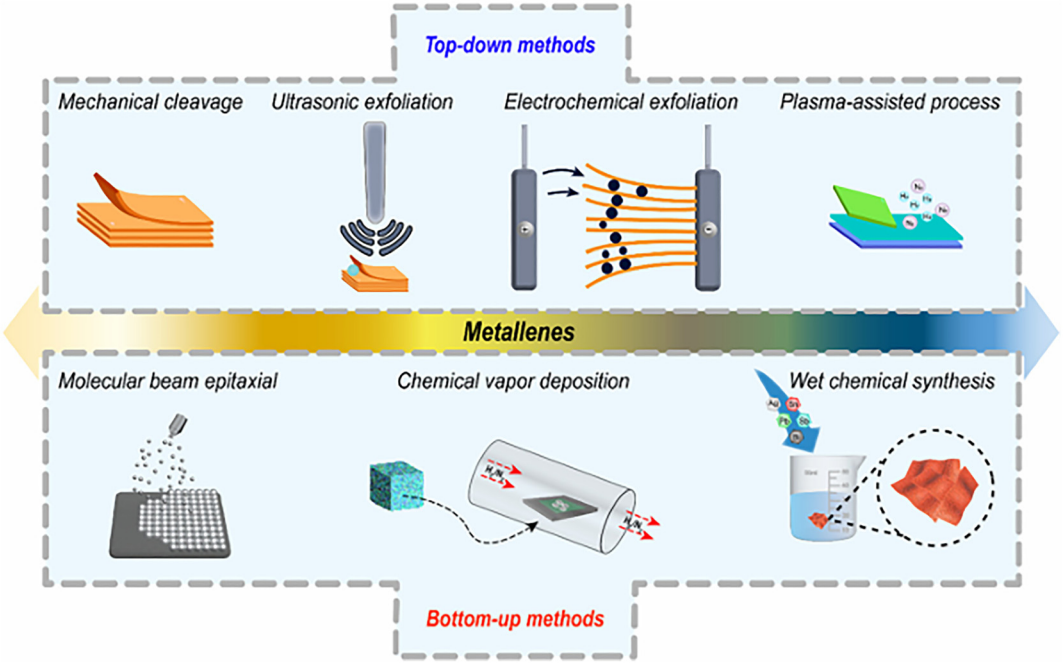

Fig. 5 Top-down and bottom-up synthesis routes of metallenes. Reproduced from ref. 15 with permission from the Royal Society of Chemistry.

to gradually add or lengthen metallene edges by regulating the reaction kinetics. The size, thickness, planarity, and crystalline phase could be adjusted to suit particular requirements by changing variables like temperature, pressure, reaction duration, solvent selection, metal precursor selection, reducing agent, and surfactant/ligand selection.

4.1. Top-down approaches

4.1.1. Mechanical cleavage. One essential technique in top-down approaches to nanomaterial synthesis, particularly for producing two-dimensional (2D) materials such as graphene, is mechanical cleavage. Using mechanical force, this approach physically breaks down bulkier materials into thinner, smaller layers. To counteract the weak van der Waals forces holding layers of atoms together in some materials, external stress is applied, for example, by rubbing, peeling, or scratching. The separation of single-layer graphene with the application of adhesive tape to peel off graphite layers is a well-known example of mechanical cleavage. The mechanical cleavage techniques are one of their main advantages. The thickness of the nanosheet can be directly controlled by varying the number of times the exfoliation process is carried out. Defect-free nanosheets are also produced using this technique, which is crucial for several applications. The mechanical cleavage method does have certain limits with regard to reproducibility and scalability. Because of its labor-intensive nature, it may not be appropriate for large-scale production and mostly depends on hand manipulation. This method is useful for research and applications needing immaculate material qualities because it can create high-quality, flawless nanosheets with little chemical contamination. Mechanical cleavage is better suited for laboratory-scale production than large-scale industrial manufacturing; nonetheless, it has limitations in terms of scalability and reproducibility.[63] For the first time, Ares *et al.* produced antimonene using the mechanical cleavage approach (Fig. 6a).[64] Scratch tape exfoliation is used to prepare the layered antimonene nanosheets (AM NSs), which are then transferred to a Si/SiO_2 substrate. To get rid of any remaining Scotch tape residue, each sample was successively cleaned with acetone, methanol, and isopropanol. Solvent residues were then eliminated by baking at 180 °C. The AM NSs with a lateral dimension of less than 240 nm and a thickness of less than 8 nm were effectively exfoliated after morphological evaluation was completed using an atomic force microscope (AFM).[65] Even though mechanical cleavage is an easy and inexpensive process, stable and predictable exfoliation requires raw bulk samples to have their own layered structure and strong in-plane connections and to be easily and affordably obtained by mechanical cleavage; however, the yield is very low.

4.1.2. Ultrasonic exfoliation. A popular top-down method for creating nanomaterials, particularly two-dimensional (2D) materials like graphene, MoS_2, and other layered compounds, is ultrasonic exfoliation. Using this method, high-frequency ultrasonic waves are used after bulk-stacked materials have been dispersed in an appropriate solvent. A process called cavitation occurs when the ultrasonic energy creates alternating waves of high and low pressure in the liquid, causing small bubbles to develop and then quickly burst. The strong local forces produced by this cavitation can separate the layers into thinner sheets or even monolayers by overcoming the weak van der Waals contacts between them. The benefits of ultrasonic exfoliation are its ease of use, affordability, and capacity to generate comparatively large amounts of exfoliated materials with little chemical alteration. However, variables like sonication

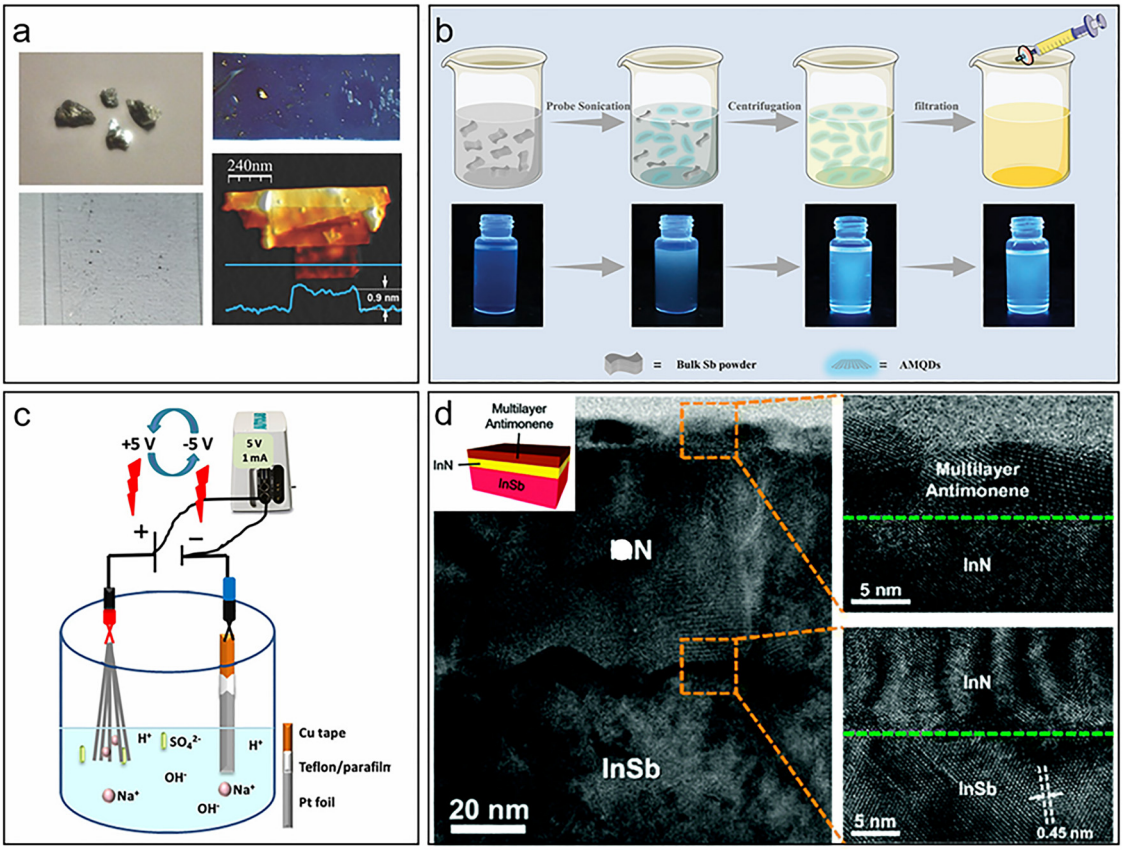

Fig. 6 Top-down strategies for the synthesis of metallenes. (a) Antimonene nanosheets prepared by mechanical cleavage, (b) schematic diagram of the preparation of antimonene quantum dots by ultrasound exfoliation, (c) general scheme for the electrochemical exfoliation of layered Sb crystals into 2D sheets, and (d) TEM image of the multilayer antimonene/InN/InSb prepared by plasma-assisted processes. Reproduced from ref. 15 with permission from the Royal Society of Chemistry.

time, solvent type, and power input can affect the final nanosheets' quality and yield. Long-term sonication can potentially cause flake size reduction or introduce flaws. Ultrasonic exfoliation is still a viable and scalable technique for creating nanomaterials in both industrial and research environments, despite these difficulties.[66]

The preparation of metallenes based on magnesium and aluminum has recently been accomplished with success. Using ultrasound exfoliation, Zhang and associates presented a unique method for low-temperature exfoliation of magnesium into 2D nanocrystals (Fig. 6b).[25] In order to alter the magnesium's slip system, they used liquid nitrogen treatment. Similarly, Lu and colleagues used ultrasound to exfoliate tiny pieces of aluminum foil into 2D aluminum sheets, which were around 1 mm in size, in ethylene glycol.[67] Additionally, Yadav *et al.* synthesized 2D metal alloys from 3D quasicrystal precursors using a scalable technique.[68] To obtain 2D structures from the decagonal quasicrystals of the bulk $Al_{66}Co_{17}Cu_{17}$ alloy, they employed robust exfoliation in a pressured ultrasonic reactor. Important effects of ultrasonic exfoliation that mostly depend on ultrasonic power and duration are the size and thickness of the resultant 2D metallene. Even though ultrasonic exfoliation has the potential to be manufactured economically and, on a large scale, there are still challenges. Currently, there is a limited yield of ultrathin 2D nanomaterials, especially monolayers. Furthermore, the solvents frequently used are hazardous organic chemicals, and the resultant nanosheets frequently lack homogeneity. The most widely used ultrasonic solvents are *N*-methyl-pyrrolidone (NMP), dimethylformamide (DMF), isopropyl alcohol (IPA), *N*-cyclohexyl-2-pyrrolidone (CHP), and dimethyl sulfoxide (DMSO). Without the use of a surfactant, Gibaja *et al.* showed that sonication could produce a stable suspension of micron-sized antimonene in a 4 : 1 isopropanol/water mixture.[69] Gusmao *et al.* described using surfactants to create bismuth nanosheets through shear exfoliation.[70] By employing IPA to crush the bulk bismuth into a powder and then using ultrasound treatment, Lu *et al.* created bismuth nanosheets.[15] Xing *et al.* ultrasonically exfoliated the bulk bismuth powder into a bismuth quantum dot dispersion using NMP as a solvent for 48 hours.[71] Then, the dispersions were passed over a porous anodic aluminum oxide membrane to gradually filter out the smaller bismuth quantum dots. Liu *et al.* used ion intercalation and ultrasound-assisted liquid phase exfoliation to create antimonene quantum dots with superior PL.[51] This synthesis process may produce a homogeneous and ultrasmall 2D material in comparison to simple probe

ultrasonography. Group VA elements bismuth, phosphorus, arsenic, and antimony exhibit both metallic and nonmetallic characteristics.

4.1.3. Electrochemical exfoliation. For the synthesis of metallenes, which are two-dimensional (2D) metallic or metal-derived nanostructures with thicknesses as low as one atomic layer, electrochemical exfoliation has become a potent and scalable method. In an electrochemical cell, this technique uses a bulk metallic or layered metal-based substance as the electrode, such as metal hydroxides, transition metal dichalcogenides, or metal foils. Electrolyte ions intercalate between the material's atomic layers when a voltage is applied, weakening metallic or van der Waals bonds through electrostatic repulsion and redox processes. The metal acts as the anode in anodic exfoliation, undergoing partial oxidation that produces gas like oxygen and intercalation ions like SO_4^{2-} and NO_3^-. In contrast, cathodic exfoliation preserves more of the intrinsic metallic structure by relying on the insertion of cations such as H^+ or Li^+ into the material when it acts as the cathode. The electrolyte selection, applied voltage, intercalation period, and temperature are important factors that affect the exfoliated metallenes' thickness, lateral size, level of oxidation, and structural integrity. Electrochemical techniques provide better control over the number of layers, lower chemical waste, and higher yields than top-down mechanical or chemical exfoliation. The resultant metallenes are intriguing candidates for use in electrocatalysis (HER, OER, and CO_2RR), batteries, supercapacitors, and nanoscale electronics because they frequently exhibit increased surface area, quantum confinement effects, and an abundance of active sites.[72] Using tiny bismuth ingots as raw materials, graphite rods as anodes, conductive copper strips as cathodes, and tetrapropylammonium bromide solution in acetonitrile as an electrolyte, Wu *et al.* carried out the electrochemical exfoliation of bismuth nanosheets in a two-electrode system.[73] Furthermore, Marzo *et al.* produced antimonene by using platinum and antimony as electrodes in Na_2SO_4 and Li_2SO_4 electrolytes at 5 V for two hours.[74] The degree and thickness of surface oxidation are influenced by the type of electrolyte and the time required to shift the voltage polarity. This offers a foundation for electrochemical exfoliation, which is used to create new, superior 2D materials. However, there are still issues with reducing structural flaws, managing oxidation conditions, and attaining consistent morphology over wide regions, all of which are major areas of continuing study to improve this technique (Fig. 6c).

4.1.4. Plasma-assisted process. Using extremely reactive plasma species, the plasma-assisted process is a sophisticated method for creating metallenes by exfoliating or converting bulk metals or metal-based compounds into atomically thin, two-dimensional layers. This process exposes a bulk precursor, usually a metal foil or layered material, to a plasma environment, which is usually created using gases like oxygen, hydrogen, or argon under high-frequency electric fields and low pressure. The materials' surface is impacted by the energetic ions, radicals, and electrons in the plasma, which causes bond breaking, etching, and surface reconstruction. The material can be selectively thinned to a few atomic layers using this controlled exposure without the use of mechanical force or chemical solvents. Power, gas type, exposure duration, and pressure are important plasma parameters that affect the final metallenes' thickness, chemical makeup, and structural integrity. Plasma-assisted synthesis provides greater control over functionalization and defect density than conventional top-down methods. It can also be utilized to insert heteroatoms or modify surface characteristics. This method is particularly appealing for applications in electrocatalysis, sensors, and nanoelectronics since the resultant metallenes frequently show increased catalytic activity, electronic conductivity, and chemical reactivity. Antimony layers were effectively synthesized by Tsai *et al.* utilizing InSb(001) substrates as templates.[75] The TEM image of the multilayer antimonene/InN/InSb prepared by plasma-assisted processes is shown in Fig. 6d. After being submerged for 30 to 60 minutes at B10 1 torr in the N_2 plasma produced by a radio frequency system (13.56 MHz) with a power of 50 to 200 W, the InSb substrates were annealed for 30 to 60 minutes at 450 °C in a N_2/H_2 (10/1, v/v) environment. Finally, the monolayer antimonene's production is visible.

4.1.5. Solid melt exfoliation. A new top-down technique for creating metallenes is called solid melt exfoliation, in which a molten medium is used to exfoliate bulk metals or stacked metal compounds into incredibly thin, two-dimensional sheets. This method involves immersing a bulk metal or metal-containing precursor at high temperatures in a molten salt or alloy solution, such as molten fluorides, chlorides, or eutectic metal combinations. Because of the significant thermal energy and chemical interactions at the interface, the molten medium functions as a solvent and a reaction environment, facilitating ion intercalation, surface diffusion, and layer separation. Few-layer or monolayer metallenes can exfoliate as a result of this process, which makes it easier for interlayer metallic or van der Waals forces to diminish. Scalability, solvent-free processing, and the possibility of doping or alloying during exfoliation are some benefits of the technique. Furthermore, high-temperature environment can decrease structural defects and enhance crystallinity, thereby improving the electrical and catalytic properties of metallenes. Solid melt exfoliation provides a new method for creating 2D metallic materials for use in high-temperature electronics, energy conversion, and catalysis. It is especially promising for creating thermally stable metallenes. Kochat *et al.* created a simple exfoliation synthesis of 2D Ga with an atomically thin layered structure from the molten phase.[76] The idea is to remove the solid layer on the surface from the solid melting interface of the low-melting metal material to create a thin layer of metal atoms. This process is anticipated to be widely used in the future to prepare a variety of gallium-based metallenes.

4.1.6. Dealloying process. Dealloying techniques are also gaining popularity, in addition to solid-melt exfoliation. In order to produce a porous, atomically thin metal nanosheet structure, metallene dealloying entails the selective removal of one or more elements from a bimetallic or multimetallic alloy.

Usually, chemical or electrochemical techniques are used to accomplish this, where a framework primarily made of the more noble metal is left behind after the less noble metal is leached off. Dealloying allows for the creation of high-surface area, defect-rich structures with improved mechanical, electrical, and catalytic capabilities in the context of metallenes, which are ultrathin, two-dimensional metal layers. Because of the process's high degree of tunable control over pore size, surface content, and thickness, dealloyed metallene materials are very appealing for use in catalysis, energy storage, and sensing. Wang *et al.* produced gold films and nanoribbons with varying single-atom thicknesses, ranging from gold to silver alloys, *via in situ* dealloying under transmission electron microscopy.[77] Under high-energy electron beams, the products, which had a minimum thickness of just 0.6 nm, were incredibly stable. Ma *et al.* created 2D stanenes with a 4 nm thickness by extracting lithium from a lithium-tin alloy (Li_5Sn_2).[78]

4.2. Bottom-up approaches

4.2.1. Molecular beam epitaxy. In the highly controlled bottom-up process known as molecular beam epitaxy (MBE), atoms or molecules of the target metals are evaporated in an ultra-high vacuum environment and then focused as beams onto a heated substrate to create metallenes. Atom by atom, the atoms build into a crystalline or epitaxial layer during this process, forming ultrathin, two-dimensional metallic structures.[79,80] MBE is suitable for creating premium metallenes with consistent atomic layers and customized features because it provides exact control over thickness, composition, and crystallinity. By successively depositing several materials, this technique also makes it possible to create heterostructures, which are essential for sophisticated applications in optoelectronics, nanoelectronics, and catalysis. Niu *et al.* directly synthesized superior 2D antimonene on a dielectric copper oxide substrate using the molecular beam epitaxy process.[81] First, a uniformly structured copper oxide surface was created using a Cu(111) single crystal. After that, Sb was deposited from a boron nitride crucible that had been thoroughly degassed onto the copper oxide surface at room temperature. Ultimately, ultrahigh-pressure annealing produced the monolayer antimonene. Wu *et al.* described a technique that uses an ultra-high vacuum chamber to manufacture antimonene on a $PdTe_2$ substrate.[82] The antimony deposited on the freshly cut $PdTe_2$ substrates was then evaporated after the $PdTe_2$ substrate was first divided to create single crystals using extremely high forces. Using solid source molecular beam epitaxy, Fortin-Deschěnes *et al.* showed how to synthesize antimonene on a germanium substrate in a scalable manner.[83] The native antimonene sheets show excellent crystal quality, semi-metallic characteristics, and stability under environmental changes, according to theoretical calculations paired with atomic-scale microscopy and spectroscopic studies. Walker *et al.* documented the direct dry transfer of molecular beam epitaxy-grown single-crystal thin films.[84] Double cantilever fracture technology was used to transfer the epitaxial bismuth film formed on silicon (111) to a silicon strip coated with epoxy resin. Electrical, optical, and structural characteristics of the transferred bismuth film were similar to those of the self-growing epitaxial film. However, in contrast to other synthesis methods, the equipment's scalability is constrained by its cost and complexity.

4.2.2. Vapor deposition technique. Metallenes, which are atomically thin 2D layers composed of metals such as Pt, Pd, Ru, or Au, can be synthesized under controlled conditions using vapor deposition techniques, including chemical vapor deposition (CVD) and physical vapor deposition (PVD).[85] These extremely thin metallic films differ from their bulk counterparts in their peculiar electrical and catalytic properties, large surface area, and quantum size effects. In CVD, a carrier gas (usually Ar, H_2, or N_2) transports volatile metal–organic or inorganic precursors (such as metal carbonyl, chlorides, or hydrides) into a reaction chamber.[86] These precursors break down or react when they come into contact with a heated substrate (often graphene, transition metal dichalcogenides, or oxides such as MgO or Al_2O_3), which causes a single or few-atom-thick metal layer to develop epitaxially or *via* van der Waals forces.[87] Nucleation density, grain size, and film continuity are controlled by carefully adjusting critical factors, including substrate temperature, gas flow rate, pressure, and precursor concentration. Tsai *et al.* used a UHV-CVD (ultra-high vacuum chemical vapor deposition) technique to create germanium nanosheets on Si(100) wafer substrates, and the annealing procedure produced thin-layered, highly crystalline germaniumene.[88] However, for metals that are hard to reduce or prone to oxidation, PVD methods like sputtering or MBE enable the atomic-level precision deposition of metallenes under ultra-high vacuum conditions. On controlled SiO_2 media substrates, Kuriakose *et al.* described a physical vapor deposition method for millimeter-scale single-phase AM NSs, as shown in Fig. 7(a–c).[89] To produce single-phase antimonene crystals or large-area nanosheets on demand, temperature gradients on the deposition tube can be employed. Furthermore, substrate engineering, which includes surface functionalization and lattice matching, is essential for stabilizing 2D metal layers that would otherwise aggregate because of their high surface energy. Recent developments have shown that stable free-standing metallenes and alloyed 2D metals with customized electronic structures can grow in the vapor phase. This opens the door to next-generation uses in flexible electronics, quantum devices, and electrocatalysis, such as the HER.

4.2.3. Wet chemical method. A flexible and scalable technique for creating metallenes, the wet chemical process, is especially helpful for creating atomically thin 2D metal nanosheets in mild environments.[90] Usually, this technique entails the chemical reduction of metal precursors in solution from the bottom up, frequently with the aid of capping agents, surfactants, or structure-directing molecules that direct anisotropic growth. Researchers can modify the lateral size, thickness, and crystallinity of the resultant nanosheets by meticulously regulating variables like precursor concentration, pH, temperature, and reaction time. For example, single-layer or few-layer metallenes of noble metals such as Pt, Pd, Au, and Ru have been synthesized using polyol synthesis, solvothermal processes, or template-assisted reduction. Lamellar micelles,

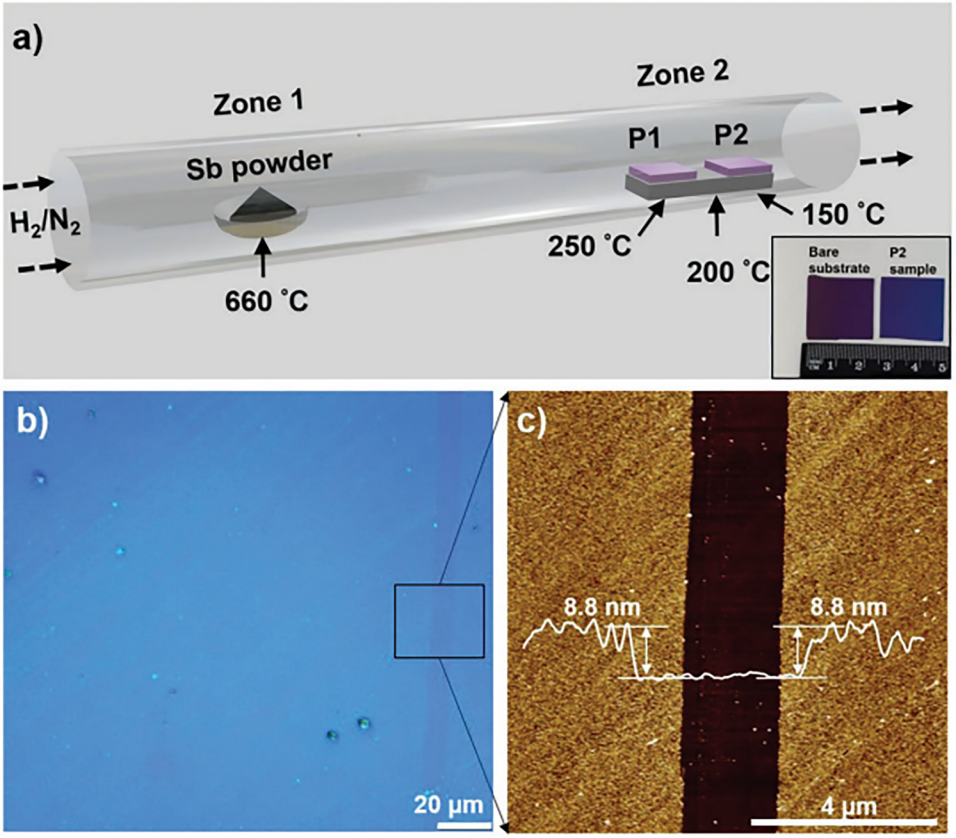

Fig. 7 (a) Schematic illustration of the synthesis process, indicating the sample positions and their respective temperatures. The inset shows an optical image of large-aspect-ratio antimonene nanosheets grown on SiO_2/Si substrate, compared with a bare SiO_2/Si substrate, (b) Microscopic image of the as-grown large-area from P2 (Position 2, in (a)), (c) Atomic force microscopy image of the area indicated in (b), with an inset showing the corresponding thickness profile. Reproduced from ref. 15 with permission from the Royal Society of Chemistry.

graphene oxide, or even layered double hydroxides are examples of 2D soft templates that are frequently employed to limit growth to two dimensions and avoid the creation of bulk or isotropic nanoparticles. Additionally, metallenes can be doped, alloyed, or functionalized during synthesis using the wet chemical technique, improving their optical, electrical, or catalytic qualities. Attaining single-crystalline domains, uniform thickness, and high phase purity at scale is still difficult, though. Despite these drawbacks, for applications in electrocatalysis, the wet chemical approach is still a flexible and affordable way to fabricate metallenes. This section provides an overview of the four typical wet chemical synthesis techniques for metallenes.

(i) Ligand confined growth: in the wet chemical synthesis of metallenes, ligand-controlled growth is a potent technique that allows for exact control over the materials' shape, thickness, and crystallographic orientation. According to this method, during nucleation and growth, organic ligands such as amines, thiols, *etc.*, bind preferentially to particular crystallographic facets of metal atoms or clusters. By changing the surface energy landscape, this selective binding effectively prevents growth in some directions while promoting 2D expansion. Small molecule ligands and organic ligands are the two general groups to which ligands belong. The redox potential of metal precursors and the surface energy of various crystalline surfaces are actively controlled by small molecule ligands, such as CO. Strong adsorbing ligands for crystal (111) facets, CO molecules, inhibit metallene development in the (111) direction. Free-standing hexagonal palladium nanosheets with a thickness of less than ten atomic layers were easily created by Huang *et al.* using carbon monoxide as a surface limiting agent.[44] The synergistic interaction of two amino ligands, dimethylacetamide (DMA) and diethylenetriamine (DETA), led Yang *et al.* to generate PtPd alloy nanosheets.[91] The concept is to employ aliphatic terminal diamines to chelate with metal precursors and slow down the reaction, while DMA adsorbs (111) crystalline surfaces selectively.

(ii) 2D templated synthesis: using a two-dimensional substance as a scaffold for controlling metal growth, the 2D template synthesis technique is employed for producing atomically thin metal nanosheets or metallenes. Graphene oxide, clay nanosheets, layered double hydroxides (LDHs), and other lamellar structures are examples of common templates. Continuous metal layers limited to two dimensions are created by introducing metal precursors onto or between the layers of the 2D template and then reducing them chemically or thermally.

Free-standing metallenes can frequently be obtained by selectively removing the template after synthesis. This method provides fine control over morphology, thickness, and lateral dimensions and is particularly helpful for generating structures with a lot of defects or strain. Fan *et al.* produced oriented Au@Ag core–shell sheets with thickness ranging from 3.0 to 4.6 nm by applying small layers of Ag on AuSSs, which caused phase transitions.[92] The synthesis of ultrathin face-centered cubic (fcc) Au@Pt rhombic nanoplates and the creation of fcc Au@Pd rhombic nanoplates were also reported by the team.[93] It is possible to apply this synthesis approach to different metallenes.

(iii) Solvothermal synthesis: it is a wet chemical process that uses organic or mixed solvents to create metallenes at high temperatures and pressures in a sealed autoclave. This method involves dissolving metal precursors in a solvent with ligands, surfactants, or structure-directing agents to direct the formation of incredibly thin 2D metal nanosheets.[94] Anisotropic growth, which favors the creation of atomically thin layers rather than bulk particles, can be achieved by carefully controlling the reaction parameters, including temperature, pressure, solvent type, and reaction time. Noble metal metallenes like Pt, Pd, and Au can be synthesized using this process, which frequently produces nanosheets with large lateral dimensions and great crystallinity.[95] Duan *et al.* used a straightforward solvothermal technique to create monolayer rhodium (Rh) nanosheets.[96] Yang *et al.* used a precursor material, $AgNO_3$/water solution stirred with glycylglycine, which offers direction for the formation of silver nanosheets, to create single-crystal silver nanoplates with tiny biomolecular guidance.[97] Thus, solvothermal synthesis is a useful method for applications in catalysis, electronics, and sensing since it enables scalable production and may be tailored for doping, alloying, or surface functionalization.

(iv) Soft colloidal templated synthesis: a bottom-up technique called soft colloidal templated synthesis uses soft templates, such as micelles, vesicles, emulsions, or surfactant assemblies, to direct the formation of ultrathin metal nanosheets. Because these soft colloidal structures limit metal nucleation and expansion to planar regions, they produce a limited, dynamic environment that enables 2D anisotropic development. Under carefully monitoring chemical circumstances, metal precursors are usually reduced *in situ* inside or near the soft template. To prevent aggregation and enable the development of ultrathin sheets, surfactants such as CTAB, PVP, or oleylamine frequently serve as stabilizers and structure-directing agents. Zhang *et al.* described creating antimonene and bismuthine nanosheets in colloidal liquids using a soft template technique (Fig. 8a–d).[98] Antimonene nanosheets with a distinct rhombohedral crystal structure could be prepared by dissolving $SbCl_3$ in alkyl phosphonic acids, which could result in a lamellar structure. This synthesis approach could potentially yield bismuthene nanosheets. By using restricted growth in micellar sheets, Xu *et al.* created ultrathin Pd NSs with a thickness of 0.8 nm and a distinctive (110) orientation plane.[99] This technique is very useful for generating noble metal metallenes like Pt, Pd, and Au with high surface area and adjustable surface characteristics. It provides good control over thickness, lateral size, and shape. The soft colloidal method is appealing for use in sensing, electrocatalysis, and biomedicine because it is mild, scalable, and adaptable. Overall, the summary of representative metallenes highlighting their synthesis methods, structural characteristics, key physicochemical properties, electrochemical performance metrics, and relative advantages

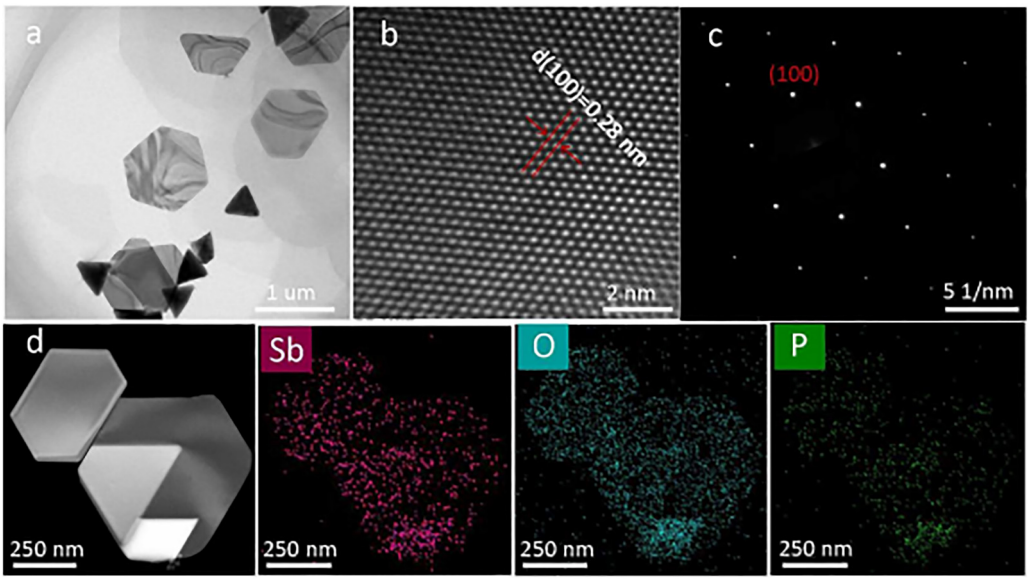

Fig. 8 (a) and (b) TEM and high-resolution TEM images of quasi-hexagonal antimonene nanosheets, (c) SAED pattern along the (001) zone axis, (d) STEM image of antimonene nanosheets and corresponding EDS mapping. Reproduced from ref. 98 with permission from the Royal Society of Chemistry.

Table 2 Summary of representative metallenes highlighting their synthesis methods, structural characteristics, key physicochemical properties, electrochemical performance metrics, and relative advantages in energy conversion and storage applications

Metallene	Synthesis method	Structural features	Key properties	Electrochemical performance	Relative advantages
Pt metallene	Wet-chemical reduction, CO-confined growth, template-assisted synthesis	Atomically thin Pt layers (<2 nm), high surface atom exposure	High conductivity, optimized d-band center, abundant unsaturated sites	ORR half-wave potential ~0.90–0.92 V *vs.* RHE (acidic media); mass activity > commercial Pt/C	Superior ORR kinetics, high mass activity, reduced noble metal usage
Pd metallene	Surfactant-directed growth, chemical exfoliation	Ultrathin Pd nanosheets with an expanded lattice	Tunable strain effect, high hydrogen adsorption affinity	HER overpotential <50 mV at 10 mA cm^{-2}; high FAOR activity	Excellent HER/FAOR performance, strong strain-induced activity enhancement
Ni metallene	Topochemical reduction, MOF-derived synthesis	Few-layer Ni sheets, porous morphology	Good electrical conductivity, abundant active sites	OER overpotential ~250–300 mV at 10 mA cm^{-2} (alkaline)	Cost-effective alternative to noble metals, good OER activity
Co metallene	Hydrothermal synthesis + reduction, electrodeposition	Atomically thin Co layers	High spin density, favorable adsorption energy for OER intermediates	OER overpotential ~280 mV at 10 mA cm^{-2}	Earth-abundant, suitable for alkaline water splitting
Fe metallene	Chemical vapor deposition (CVD), solution-phase reduction	Ultrathin Fe layers with a defect-rich surface	Strong electronic interaction with supports	Enhanced OER performance when hybridized with Ni/Co	Low cost, synergistic effect in bimetallic systems
PtNi metallene	Seed-mediated growth, alloying + dealloying	Alloyed 2D structure with lattice strain	Modified d-band center, improved adsorption/desorption balance	ORR mass activity 10–20× commercial Pt/C	Exceptional ORR activity and durability
PdMo metallene	Wet-chemical co-reduction	Strain-engineered bimetallic nanosheets	Synergistic electronic coupling	High HER activity in acidic/alkaline media	Improved stability and catalytic kinetics
Rh metallene	Surfactant-assisted chemical reduction	Atomically thin Rh layers	Strong hydrogen adsorption capability	Low HER overpotential (~20–30 mV)	Excellent HER catalyst with minimal thickness

in energy conversion and storage applications is presented in Table 2.

5. Characterization

An in-depth understanding of the formation mechanism, structural evolution, and functional features of metallenes requires improved characterization techniques that can investigate their ultrathin thickness, elevated surface energy, and metastable characteristics. In contrast to bulk metals, metallenes, which are frequently composed of single-atom or few-atom thickness, are highly vulnerable to thermal fluctuations, electrochemical conditions, and electron beam irradiation. These factors can cause rapid atomic arrangements, phase transformations, or even structural collapse. To clarify their nucleation behavior, anisotropic growth, alloy distribution, and structure–property relationships governing electronic and catalytic performance, a combination of *in situ*/*operando* characterization tools, high-resolution microscopy, surface-sensitive spectroscopy, and computational simulations is crucial.[100] Schematic illustrations of a multimodal characterization workflow for metallenes, integrating *in situ* techniques, microscopy, spectroscopy, and theoretical modeling, are shown in Fig. 9.

5.1. *In situ* and *operando* characterization

5.1.1. *In situ* transmission electron microscopy (TEM). Under realistic reaction conditions, *in situ* TEM is essential for directly observing the nucleation, growth kinetics, and real-time structural evolution of metallenes. Using this method, near-atomic resolution observations of edge reconstruction, atomic migration, lattice distortion, strain-field evolution, and defect dynamics are made possible. However, metallenes are extremely beam-sensitive because of their single-atom thickness; with extended electron exposure, they frequently experience amorphization, perforation, or disintegration. Low-dose imaging techniques and cryogenic TEM (cryo-TEM), which greatly preserve intrinsic lattice integrity while permitting atomic-scale investigation, have been widely used to lessen these effects.[101] *In situ* TEM snapshots depicting metallene nucleation, lateral growth, and edge reconstruction under controlled reaction conditions are displayed in Fig. 10.

5.1.2. *In situ* X-ray diffraction (XRD). The schematic picture of *in situ* GI-XRD monitoring lattice evolution during metallene growth is shown in Fig. 11. During metallene synthesis or heat treatment, *in situ* XRD offers real-time insights into phase evolution, lattice expansion or contraction, strain relaxation, and crystallization paths.[102] Grazing-incidence XRD (GI-XRD) is especially useful for detecting weak diffraction signals from two-dimensional metallic layers and improving surface sensitivity due to the ultrathin nature of metallenes.

5.1.3. *In situ* Raman spectroscopy. A non-destructive method for monitoring vibrational modes, strain effects, phonon confinement, and phase transitions during metallene production or catalytic activity is Raman spectroscopy.[103] Raman spectroscopy is particularly helpful for *operando* research under electrochemical circumstances because shifts in Raman peak

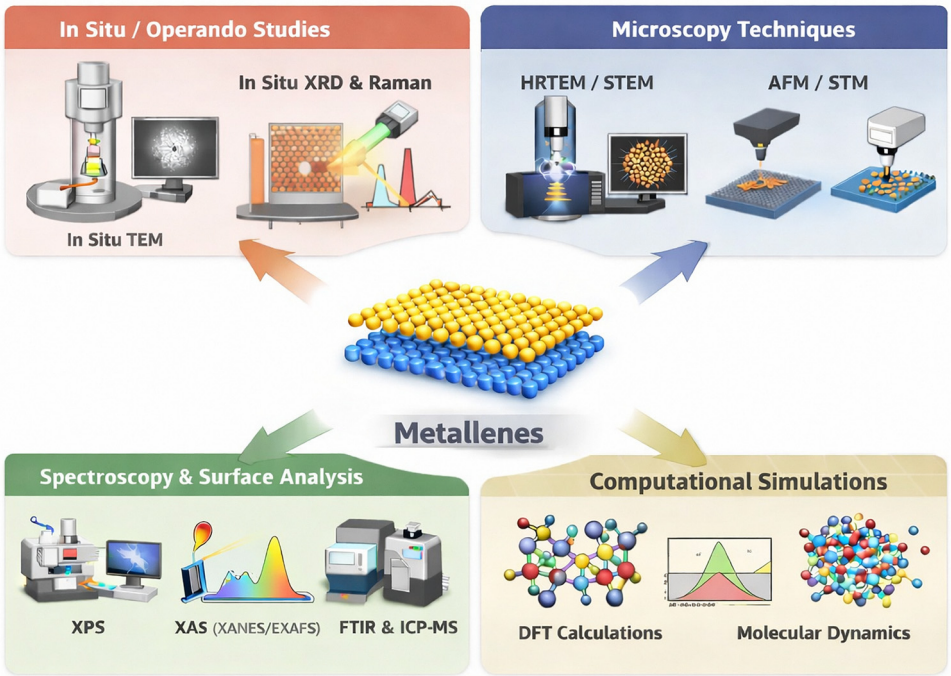

Fig. 9 Schematic illustrations of a multimodal characterization workflow for metallenes, integrating *in situ* techniques, microscopy, spectroscopy, and theoretical modelling.

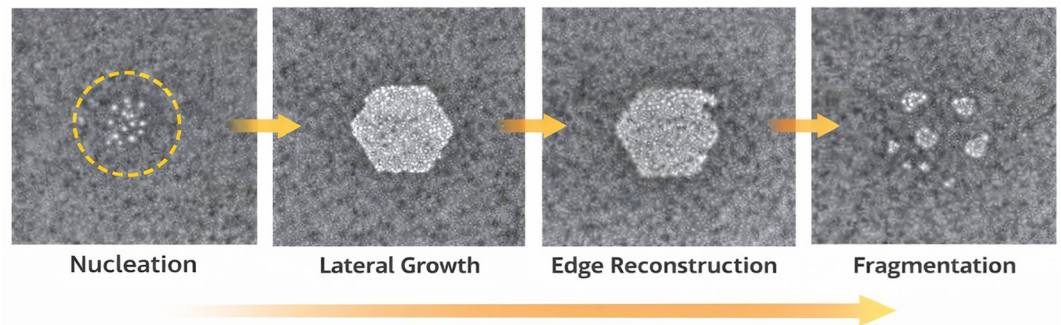

Fig. 10 *In situ* TEM snapshots depicting metallene nucleation, lateral growth, and edge reconstruction under controlled reaction conditions.

positions and variations in linewidths offer indirect evidence of lattice deformation, defect generation, and electronic coupling.

5.1.4. *In situ* X-ray absorption spectroscopy (XAS). For examining the oxidation states, coordination environment, and local bonding configuration of metal atoms in metallenes, *in situ* and *operando* XAS, such as X-ray Absorption Near Edge Structure (XANES) and Extended X-ray Absorption Fine Structure (EXAFS), are effective techniques.[104] During catalytic processes, *operando* XAS is especially useful for revealing dynamic alloy rearrangement, active-site reconstruction, and reaction intermediates.[105] The *operando* XAS analysis correlating coordination changes with catalytic activity is displayed in Fig. 12.

5.2. Microscopy techniques

5.2.1. High-resolution-TEM (HRTEM) and aberration-corrected TEM. Lattice fringes, crystallographic orientation, dislocations, point defects, and domain boundaries within metallenes can all be seen at the atomic scale using an HRTEM. Single metal atoms and edge terminations can now be directly imaged by the development of aberration-corrected TEM, which has further enhanced spatial resolution.[106] However, beam-induced stability is still a significant problem that calls for additional methods and ideal imaging conditions.

5.2.2. Scanning TEM (STEM: HAADF, BF, EDS, and EELS). STEM-based methods provide comprehensive structural and chemical insights. Z-contrast imaging is made possible by high-angle annular dark-field (HAADF) STEM, which enables the distinction between alloying elements in bimetallic or multimetallic metallenes. Elemental mapping and electronic structure investigation are made easier by energy-dispersive X-ray spectroscopy (EDS) and electron energy-loss spectroscopy

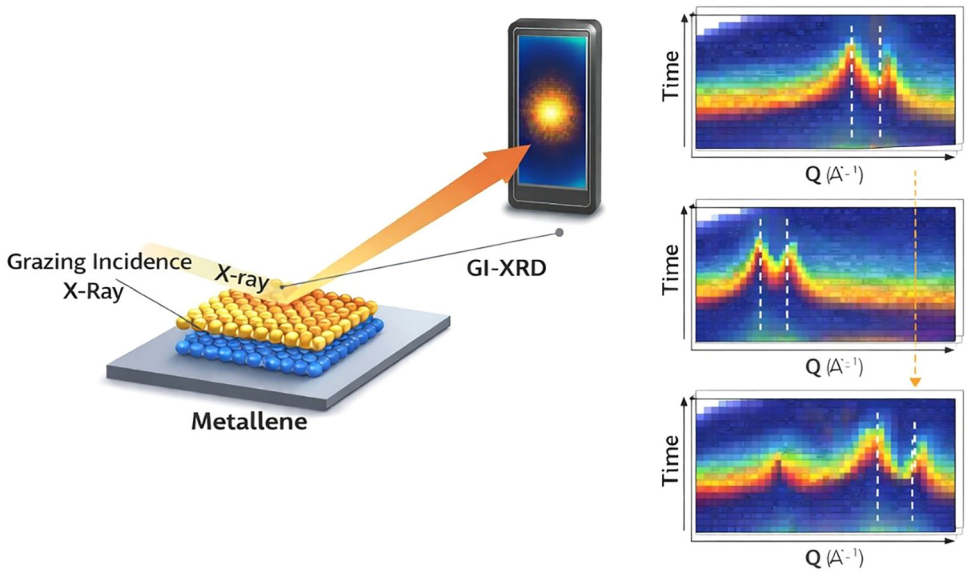

Fig. 11 A schematic picture of *in situ* GI-XRD tracking lattice evolution during metallene growth.

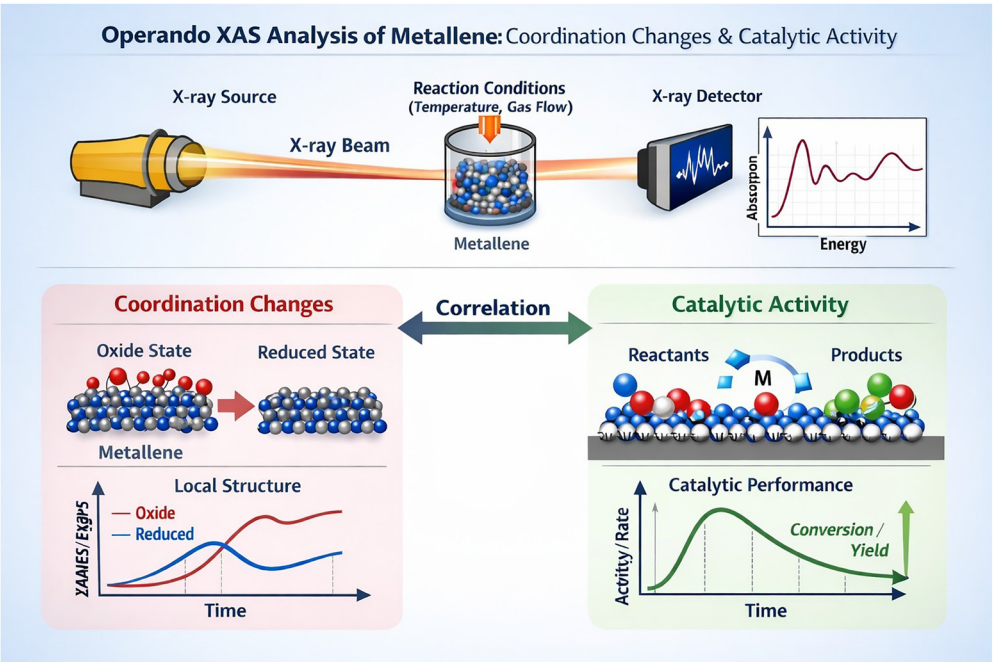

Fig. 12 *Operando* XAS analysis correlating coordination environment changes with catalytic activity.

(EELS). Cryo-STEM has become a successful method for chemically sensitive metallenes to reduce atom migration and beam damage.[107] HAADF-STEM and EDS elemental maps highlighting alloy distribution in a bimetallene are presented in Fig. 13.

5.3. Surface chemical characterization

X-ray photoelectron spectroscopy (XPS) is a commonly used technique to determine the bonding topologies, oxidation states, and surface composition of metallenes. Angle-resolved XPS (ARXPS) is especially helpful for investigating depth-dependent chemical changes and surface reconstruction phenomena in ultrathin metallic films because of their exceptional surface sensitivity.[108]

5.3.1. Fourier transform infrared (FTIR) spectroscopy. Finding surface ligands, adsorption intermediates, and metal–ligand interactions, particularly in chemically or colloidally produced metallenes, requires the use of FTIR spectroscopy. This understanding is crucial for comprehending catalytic behavior and surface stabilization processes.[109]

5.3.2. ICP-OES and ICP-MS. Complementing surface-sensitive techniques and guaranteeing compositional reliability,

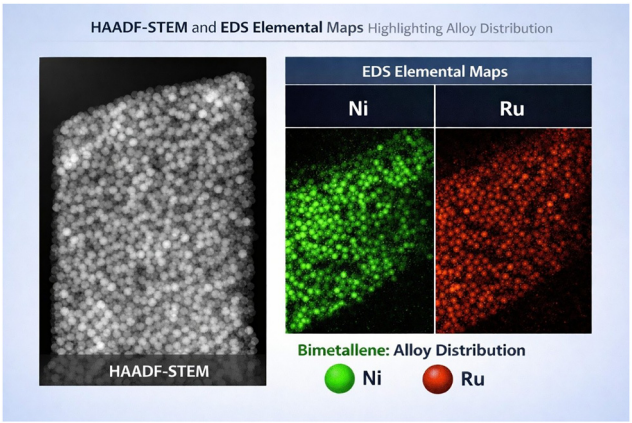

Fig. 13 HAADF-STEM images and corresponding EDS elemental maps, highlighting the spatial alloy distribution within the bimetallene.

inductively coupled plasma techniques offer precise quantitative analysis of metal content and alloy stoichiometry.[110]

5.4. Morphological and topographical characterization

5.4.1. Atomic force microscopy (AFM). Surface roughness, nanoscale shape, and metallene thickness (monolayer *versus* few-layer) may all be precisely measured by AFM. The assessment of nanomechanical characteristics, such as modulus, adhesion, and flexibility, which are essential for flexible and wearable electronic devices, is further made possible by advanced AFM modes.[111]

5.4.2. Scanning tunnelling microscopy (STM). Atomic structure, defects, edge states, and electrical characteristics can be directly correlated with the STM's atomically detailed surface imaging and access to the local density of states (LDOS). STM studies are very useful for investigating surface reconstruction processes and quantum confinement effects.[112] AFM height profiles and STM atomic-resolution images of a monolayer of metallenes are shown in Fig. 14.

5.5. Optical spectroscopy

5.5.1. UV-vis-NIR spectroscopy. Quantum confinement effects, plasmonic resonances, and alloy-induced electronic transitions in two-dimensional metals are all studied using UV-vis-NIR spectroscopy. Variations in absorption characteristics reveal information about compositional tuning, electronic coupling, and thickness variation.[113]

5.5.2. Photoluminescence (PL) spectroscopy. While bulk metals are generally non-luminescent, some metallenes show photoluminescence due to ligand-induced states, surface defects, or quantum size effects. Thus, PL spectroscopy is a sensitive probe for defect-mediated recombination processes and electron–phonon coupling.[114]

5.6. Mechanical, thermal, and stability analysis

5.6.1. Nanoindentation and AFM-based nanomechanics. For strain-engineered devices and flexible electronics, quantifiable data on Young's modulus, fracture behavior, flexibility, and strain tolerance can be obtained through mechanical characterization utilizing nanoindentation or AFM-based force spectroscopy.[115]

5.6.2. Thermal analysis (TGA/DSC). Differential scanning calorimetry (DSC) and thermogravimetric analysis (TGA) provide assistance for processing and device integration by revealing ligand desorption temperatures, thermal stability windows, and decomposition paths.[116]

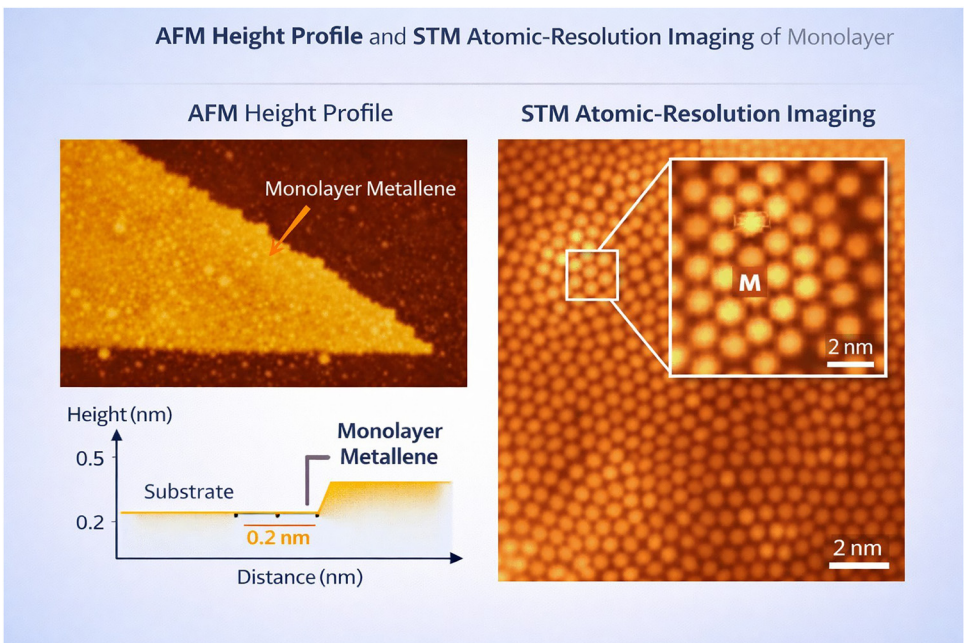

Fig. 14 AFM height profiles and atomic-resolution STM images of a metallene monolayer.

5.7. Computational simulations

5.7.1. Density functional theory (DFT). For the prediction of growth energetics, defect formation energies, electronic band structure, adsorption energies, and catalytic reaction pathways, DFT simulations are essential.[117] Additionally, DFT is essential for anticipating metastable metallene phases that cannot be accessed by direct synthesis and for interpreting experimental findings from XAS, Raman, and TEM. The synergistic integration of experimental characterization and computational modeling in metallene research is summarized in Fig. 15.

5.7.2. Molecular dynamics (MD) simulations. By offering time-resolved insights into thermal stability, atomic diffusion, mechanical deformation, and fracture dynamics under practical operating conditions, MD simulations supplement DFT.[118]

6. Applications

The exceptional physicochemical characteristics of metallenes, including high electrical conductivity, abundant active sites, tunable surface chemistry, and quantum size effects, have opened up novel prospects in various technological fields. As a whole, metallenes outperform traditional nanostructured metals or other two-dimensional materials in terms of electron transport and catalytic kinetics due to their atomic-scale thickness and metallic bonding. Furthermore, the aforementioned traits have established them as multifunctional platforms for electrocatalysis and energy storage applications. Hence, this section systematically analyses the various uses of metallenes, with an emphasis on their structure–property connections and current performance breakthroughs.

6.1. Electrocatalysis

Electrocatalysis is one of the most actively explored areas for metallenes, owing to their inherent metallic conductivity, atomic-scale thickness, and abundance of active surface atoms. The ultrathin structure of metallenes maximizes the exposure of catalytic sites, enabling efficient adsorption and activation of reactant molecules. Meanwhile, the metallic bonding network ensures rapid charge transfer across the nanosheet plane. Unlike conventional metal nanoparticles or bulk catalysts, metallenes offer a unique combination of high electrical conductivity, tunable surface energy, and quantum size effects, which collectively upsurge catalytic kinetics and reaction selectivity. Overall, these advantages make metallenes highly promising for key energy-conversion reactions such as the hydrogen evolution reaction (HER), oxygen evolution reaction (OER), oxygen reduction reaction (ORR), carbon dioxide reduction reaction (CO_2RR), and nitrogen reduction reaction (NRR).

In the case of HERs, metallenes have displayed an exceptional activity due to their exposed, under-coordinated atoms and reduced diffusion barriers for proton adsorption and desorption. For example, noble metal metallenes, such as Pt, Ru, and Pd, exhibit exceptional HER activity, surpassing their bulk or nanoparticle counterparts in both efficiency and stability.[19] Ru metallene nanobelts (RuMNs) achieved an

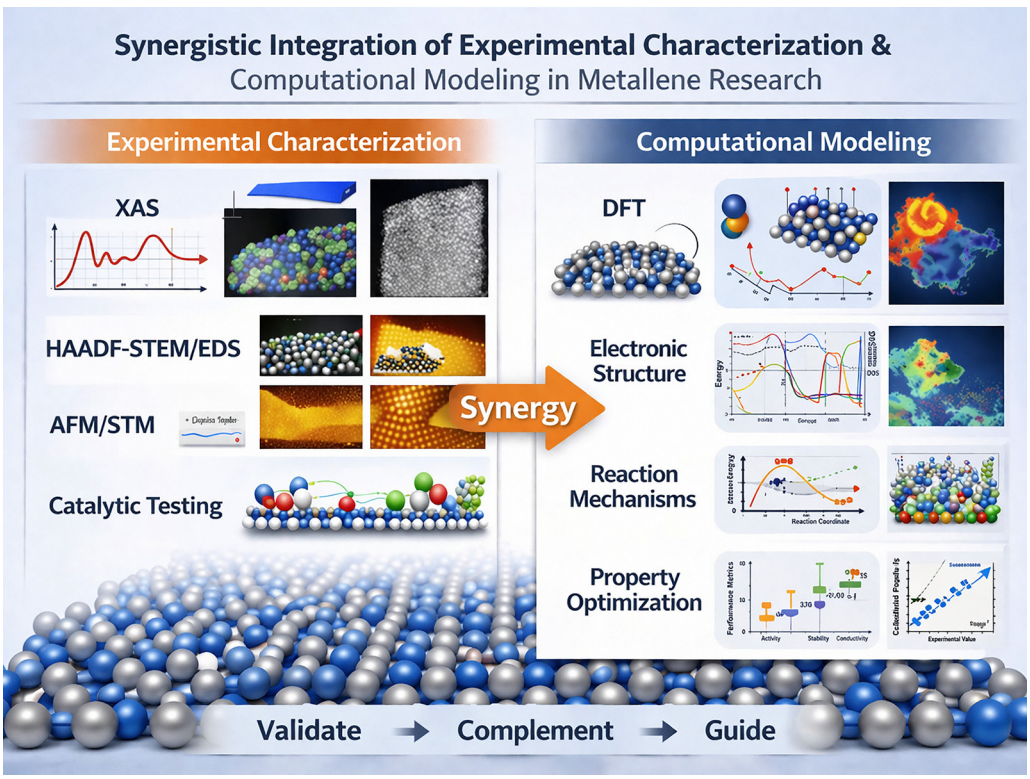

Fig. 15 A summary of the complementary roles of experimental characterization and computational modeling in elucidating the properties and performance of metallenes.

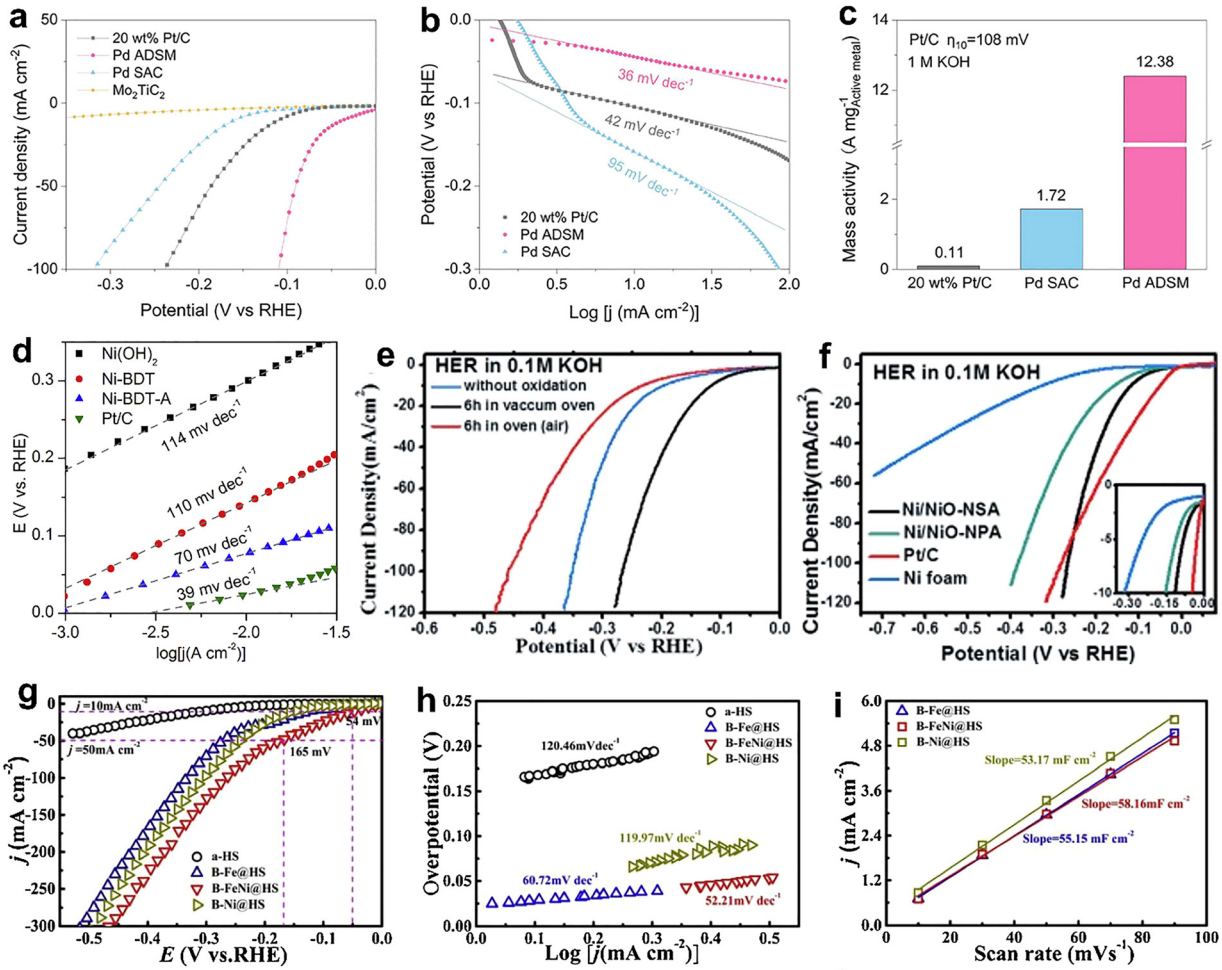

Fig. 16 HER performances. (a) HER polarization curves of different materials in 1 M KOH. (b) Tafel plots obtained from the HER curves. (c) Mass activity comparison of the materials in 1 M KOH. Reproduced from ref. 119 with permission from Wiley, Copyright 2025. (d) Tafel plot of $Ni(OH)_2$, Ni-BDT, Ni-BDT-A, and Pt/C. Reproduced from ref. 121 with permission from Elsevier, Copyright 2017. (e) HER performance of Ni/NiO-NSAs under various conditions. (f) HER polarization curves of Ni/NiO-NSAs, Ni/NiO-NPA, Ni foam, and commercial Pt/C. Reproduced from ref. 122 with permission from Wiley, Copyright 2017. (g) HER polarization curves, (h) Tafel plots, and (i) double-layer capacitance in 1.0 M KOH of a-HS, B-Fe@HS, B-Ni@HS, and B-FeNi@HS. Reproduced from ref. 124 with permission from Elsevier, Copyright 2021.

ultra-low overpotential of 19 mV at 10 mA cm^{-2} and a Tafel slope of 28 mV dec^{-1}, outperforming commercial Pt/C while remaining stable over 100 hours. Furthermore, the Pd ADSM catalyst demonstrated excellent performance, with an overpotential of 36 mV at 10 mA cm^{-2}, a Tafel slope of 36 mV dec^{-1}, and increased mass activity (12.38 A mg^{-1} Pd), outperforming both Pd SAC and Pt/C, which can be seen in Fig. 16(a–c), and remaining stable for 70 hours.[119] Meanwhile, Ru-ene superlattices exhibited similar HER activity, with an overpotential of 50 mV and a Tafel slope of 42.38 mV dec^{-1}.[120] Platinum is still used as both a standard and a core material in metallene catalysts; Pt metallenes, with high surface-to-volume ratios and numerous active sites, form extremely efficient catalytic centres. Theoretical studies frequently use Pt(111) as a reference, indicating that tailored Ru and Pd metallenes can reach even more favourable HER kinetics by defect formation, strain control, and ligand engineering.[8] Overall, these findings demonstrate that noble metal metallenes have outstanding catalytic efficacy and durable stability, making them extremely promising electrocatalysts for hydrogen evolution.

More importantly, earth-abundant metallenes based on Ni, Co, and Fe have emerged as low-cost, long-term alternatives to noble-metal systems, providing variable catalytic activity *via* compositional and structural engineering. For instance, ultrathin Ni nanosheets derived from Ni-thiolate precursors revealed high HER activity, necessitating overpotentials of 80 mV at 10 mA cm^{-2} and 150 mV at 100 mA cm^{-2}, with a Tafel slope of 70 mV dec^{-1} (Fig. 16d).[121] Similarly, partially oxidized Ni/NiO nanosheet arrays achieved an onset potential of −34 mV in 0.1 M KOH, with a Tafel slope of 114 mV dec^{-1}, as displayed in Fig. 16(e and f). The lower energy barrier for H_2 desorption on Ni/NiO(111) compared to pure Ni(111) surfaces highlights the role of surface oxygen species in enhancing the HER kinetics. The integration of trace surface sulfide ($S^{-}_{a}d$) species enhanced water dissociation and facilitated the movement of H_ad intermediates, underscoring the impact of

heteroatom modification on Ni-based metallenes.[122] In terms of cobalt, Co nanosheet arrays demonstrated remarkable HER activity in alkaline medium, delivering 10, 100, and 400 mA cm^{-2} at overpotentials of 20, 60, and 83 mV, respectively, with a low Tafel slope of 42.6 mV dec^{-1}, outperforming commercial Pt/C catalysts. The high double-layer capacitance (1.40 F cm^{-2}) and low charge-transfer resistance (1.5 Ω cm^2) validated the huge active surface area and effective electron transfer.[123] Furthermore, the addition of phosphorus was recognized as crucial in enhancing the catalytic sites. Moreover, boron-doped Fe–Ni solid-solution nanosheets (B–FeNi@HS) displayed exceptional bifunctional catalytic performance for both the HER and the OER, obtaining an overpotential of 54 mV at 10 mA cm^{-2} and a Tafel slope of 52.2 mV dec^{-1}, with long-term operational stability up to 500 mA cm^{-2} for 72 hours, as shown in Fig. 16(g–i).[124] Overall, these findings confirm that rational defect engineering, heteroatom doping, and alloying in earth-abundant metallenes efficiently modify electronic structures and hydrogen binding energies, resulting in catalytic performance comparable to or superior to that of precious metal equivalents.

Regarding oxygen-related reactions (OER and ORR), metallenes exhibit a significant advantage owing to their metallic nature and atomic thickness. Metallenes accelerate the slow multi-electron transfer processes that normally limit these reactions due to their high density of active surface sites and efficient electron transport channels, as shown in Fig. 17a. For instance, a 2D Ir–Fe/IrO_2 metallene catalyst is a highly efficient system for the oxygen evolution reaction (OER), exhibiting excellent activity and durability. The Ir–Fe/IrO_2 catalyst achieves 10 mA cm^{-2} in 0.5 M H_2SO_4 with an overpotential of only 220 mV, beating commercial Ir/C (300 mV) and IrO_2 (280 mV) benchmarks. Furthermore, the low Tafel slope of 48.5 mV dec^{-1} indicates rapid OER kinetics, while the material exhibits outstanding stability, maintaining its performance for over 100 hours with only a 10 mV rise in overpotential after 10 000 cycles. The

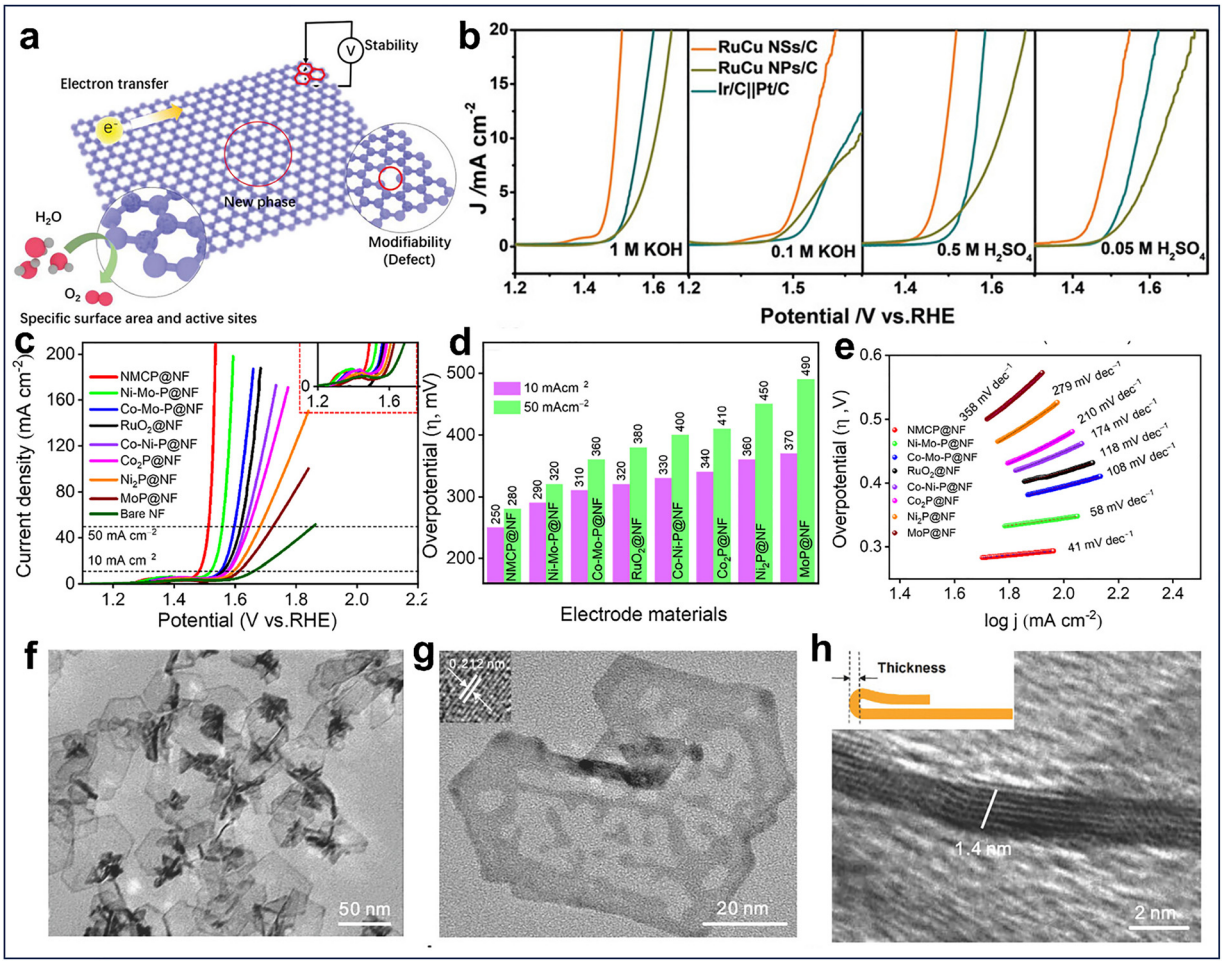

Fig. 17 OER performances. (a) Advantages of metallenes for electrocatalysis applications. Reproduced from ref. 125 with permission from Wiley, Copyright 2023. (b) LSV profiles of RuCu NSs/C, RuCu NPs/C and Ir/CkPt/C for overall water splitting applications. Reproduced from ref. 127 with permission from Wiley, Copyright 2019. (c) LSV profiles, (d) comparative overpotentials, and (e) Tafel plots values of NMCP@NF, Ni–Mo–P@NF, Co–Mo–P@NF, RuO_2@NF, Co–Ni–P@NF, Co_2P@NF, Ni_2P@NF, and MoP@NF. Reproduced from ref. 130 with permission from Elsevier, Copyright 2022. (f) TEM and (g) and (h) HRTEM images of the ultrathin $Pt_{32}Pd_{48}Ni_{20}$ NSs at different magnifications. Reproduced from ref. 132 with permission from Wiley, Copyright 2019.

synergistic interaction between Ir and Fe atoms enhances the electronic structure of IrO_2, facilitates the participation of lattice oxygen, and accelerates the formation of highly active Ir–O species, resulting in excellent performance. Moreover, Fe inclusion minimizes noble metal usage, promotes charge redistribution, and regenerates active sites, making Ir–Fe/IrO_2 metallenes an optimal design for acid-stable and high-efficiency OER catalysts.[125]

In comparison to Ir-based metallenes, Ru-based metallenes have demonstrated excellent bifunctional activity for both the HER and the OER across various pH conditions. The Ru–Ni nanosheets produced using a surfactant-assisted approach achieved 10 mA cm^{-2} for both the HER and the OER in 1 M KOH, with a Tafel slope of 32 mV dec^{-1} and excellent durability over 20 hours. The addition of Ni enhanced Ru's electrical structure allows for faster charge transfer and more effective intermediate adsorption.[126] Furthermore, Ru–Cu nanosheets with crystalline Ru and amorphous Cu domains exhibited pH-universal water-splitting activity, achieving a current density of 10 mA cm^{-2} at low voltages (1.49–1.55 V) in both acidic and alkaline electrolytes, as shown in Fig. 17b. Their low overpotentials (19–27 mV for the HER and 234–240 mV for the OER) and stability after 45 hours were linked to synergistic Ru–Cu interactions and a porous nanosheet framework that facilitated electron and ion transport.[127] Finally, Ru–Ni and Ru–Cu metallenes outperform Ir–Fe/IrO_2 in the acidic OER, demonstrating their catalytic adaptability across all pH ranges. This highlights Ru-based 2D structures as efficient and lasting options for water-splitting systems.

Furthermore, earth-abundant transition-metal-based metallenes, such as NiFe, CoNi, and FeCo, have emerged as viable and environmentally friendly alternatives for the oxygen evolution reaction. The synergistic interaction of different metal centers in these bimetallic systems promotes charge redistribution and optimizes the adsorption–desorption energies of oxygen intermediates, thereby reducing overpotentials and enhancing reaction kinetics. For instance, NiFe layered double hydroxide nanosheets outperformed monometallic Ni or Fe catalysts in terms of OER activity, with an overpotential of ~240 mV at 10 mA cm^{-2} and a small Tafel slope of 48 mV dec^{-1}, attributed to rapid electron transport and increased active site density.[128] Similarly, CoNi and CoFe heterostructures exhibited effective charge transport and a high density of edge-exposed active sites. Furthermore, the Fe-incorporated Co-based MOF ultrathin nanosheets demonstrated a low overpotential of 297 mV at 10 mA cm^{-2} and a Tafel slope of 50 mV dec^{-1}, even surpassing those of RuO_2. The hybridized bimetallic phosphides, including Ni–Mo–P, Co–Mo–P, and Co–Ni–P, attained overpotentials of 88 mV (HER) and 250 mV (OER) at 10 mA cm^{-2} as shown in Fig. 17(c–e), demonstrating their efficiency in water splitting.[129,130] Altogether, the combined findings from these systems demonstrate that adjusting electronic structures *via* alloying or hybridization significantly improves catalytic activity, bridging the performance gap between precious-metal catalysts and earth-abundant metallenes for efficient water electrolysis.

Building on the OER-active Ir- and Ru-based metallenes, Pt-based systems have been substantially tuned for the oxygen reduction reaction (ORR), which is critical in fuel cell cathodes. The ultrathin Pt-based multimetallic nanostructures, particularly those incorporating transition metals such as Ni, Co, or Fe, have demonstrated extraordinary behaviour and endurance due to electrical modulation and strain effects. For instance, Lai *et al.* found that Pt–M (M = Fe, Co, Ni) alloyed ultrathin nanowires and nanosheets shifted the Pt d-band centre, reducing oxygen adsorption and enhancing ORR kinetics. Furthermore, the PtNiCo nanowires exhibit a remarkable mass activity of 4.20 A mg^{1} Pt at 0.9 V *vs.* RHE, which is approximately 32 times greater than that of commercial Pt/C, with minimal decay after 30 000 cycles. Similarly, ultrathin PtPb nanoplates and Pt_3Ni nanoframes provided substantial active surface exposure (Fig. 17(f–h)), resulting in improved mass activities of up to 4.3 A $mgPt^{-1}$ with excellent stability.[131] Furthermore, Lai *et al.* developed ultrathin PtPdM (M = Ni, Fe, Co) nanosheets (~1.4 nm thick), combining 2D shape and multimetallic composition for excellent bifunctional performance. Among them, $Pt_{32}Pd_{48}Ni_{20}$ nanosheets outperformed commercial Pd/C and Pt/C, with an ORR mass activity of 0.54 A mg $(Pt + Pd)^{-1}$ at 0.9 V and negligible degradation after 10 000 cycles. The improved performance results from synergistic effects of ligand and lattice strain, which promote effective oxygen adsorption and desorption, as well as charge redistribution.[132]

Apart from this, FePt metallenes have also emerged as effective bifunctional ORR catalysts due to the strong electronic interaction between Fe and Pt atoms, which enhances charge redistribution and oxygen intermediate adsorption. The FePt nanosheets with nearby Pt sites (~6.7 wt%) had a high ECSA of 545.54 m^2 $g_{Pt}{}^{-1}$ and approximately seven times higher mass activity than commercial Pt/C. They used a four-electron route with exceptional CO tolerance (only 5% current loss at 10% CO) and maintained 73.9% mass activity after 20 000 cycles. The DFT research indicated that Fe inclusion lowers the Pt d-band center, weakens Pt–CO bonding, and increases OH adsorption, enhancing activity and durability. Overall, Fe inclusion effectively modifies Pt's electronic structure, producing a highly active, CO-tolerant, and long-lasting ORR catalyst.[133]

Beyond water splitting, metallenes have recently been utilized in carbon dioxide reduction (CO_2RR) and nitrogen fixation (NRR) processes, where surface atomic coordination serves a vital role in regulating catalytic selectivity. The quantity of exposed active sites in these ultrathin frameworks enhances CO_2 adsorption and stabilizes critical intermediates, thereby increasing the selectivity toward products such as CO, formate, and hydrocarbons. For instance, Cu-based metallenes exhibit excellent activity and product tunability, with 2D-Cu nanosheets displaying a faradaic efficiency (FE) of 92% for CO production at −0.7 V *vs.* RHE ascribed to plentiful Cu^0/Cu^+ interfacial sites that favour CO_2 activation. Similarly, Pd-based metallenes reached a 95% FE for formate at −0.6 V *vs.* RHE, allowing for large current densities to be maintained over long periods of time with minimal deterioration. On the other hand, Sn-based metallenes favoured the formate pathway,

achieving an FE of 89% at −0.9 V *vs.* RHE and maintaining remarkable stability for 20 hours. Furthermore, bimetallic systems, such as Ni–Cu and Ag–Bi, exhibit synergistic actions that balance hydrogen evolution suppression with CO_2RR selectivity, enabling the synthesis of multi-carbon products at modest overpotentials.[134]

Building upon the structural benefits of metallenes for CO_2 reduction, recent studies suggest that selectivity and activity are controlled by tuning defect density and morphology in various systems. For instance, hierarchical Cu nanosheets produced using a galvanic replacement technique had a partial current density of 23.0 mA cm^{-2} at −1.0 V *vs.* RHE and a faradaic efficiency (FE) of 74.1% for CO production. The remarkable performance is attributed to hierarchical porous architectures and vacancy defects that stabilize CO intermediates and facilitate charge/mass movement.[135] Similarly, ultrathin Pd nanosheets undergo surface reconstruction from (111) to (100) facets, which significantly improves CO selectivity to 93% at −0.7 V *vs.* RHE with a site-specific activity of 6.6 mA cm^{-2} due to the exposure of more active sites and optimized CO binding strength.[136] In contrast, Bi-based metallenes dominated the formate pathway, delivering up to 91% conversion at low overpotentials due to their electron-rich layered structure and high adsorption energy for OCHO intermediates. In contrast, Ni metallenes, with numerous defect sites and favourable d-band alignment, demonstrated effective CO_2-to-CO conversion, achieving faradaic efficiency exceeding 85% and exhibiting strong operational stability.[137,138] Collectively, these findings show how the catalytic pathway and product selectivity in the CO_2RR are determined by atomic-level control over thickness, facet orientation, and defect distribution in 2D metallene frameworks, providing a flexible design platform for next-generation carbon-neutral electrocatalysts.

In a similar vein, few-layered Fe, Mo, and Ru metallenes have demonstrated potential in N_2 fixation, enabling the conversion of nitrogen to ammonia under ambient conditions with higher faradaic efficiency than standard catalysts. Among these, Mo-based metallenes exhibit a remarkable affinity for nitrogen due to their d-electron configuration, which resembles that of biological nitrogenase centres. For example, Mo single atoms anchored on N-doped porous carbon achieved an NH_3 yield of 34.0 μg h^{-1} mg_{cat}^{-1} and a faradaic efficiency (FE) of 14.6%, whereas Mo_0/GDY catalysts displayed better efficiency with an NH_3 yield of 145.4 μg h^{-1} mg_{cat}^{-1} and an FE of 21.0% under ambient conditions.[139] Similarly, Fe-based metallenes achieved increased N_2 fixation by synergistic Fe–N coordination, yielding an NH_3 production rate of 32.8 μg h^{-1} mg_{cat}^{-1} and FE of 19.5%. Theoretical evidence suggests that Fe sites efficiently weaken the N≡N bond *via* back-donation mechanisms.[140]

Meanwhile, Ru-based nanosheet metallenes possess superior intrinsic activity, with an NH_3 yield of 38.2 μg h^{-1} mg_{cat}^{-1} and FE of 23.4% at −0.3 V *vs.* RHE, attributed to the optimized Ru–N bond strength, which allows for intermediate stabilization while suppressing the hydrogen evolution reaction (HER).[141] Additionally, Rh-based metallenes are highly effective at reducing N_2 due to their amorphous-crystalline hybrid structure, which provides several low-coordinated sites for activation. The Rh nanosheet catalyst had a high NH_3 production of 41.3 μg h^{-1} mg_{cat}^{-1} and a faradaic efficiency of 26.7% at −0.25 V *vs.* RHE, with steady performance for 15 hours.[142] The Pd–MoNi–Co metallene, with a multimetallic synergy and defect-rich 2D framework, achieved an excellent NH_3 production of 58.6 μg h^{-1} mg_{cat}^{-1} and FE of 31.2%, attributable to optimized d-band alignment and rapid charge transfer.[143] These findings highlight the potential of metallenes to host distinct active sites that drive multistep reactions with complex adsorbate species, making them ideal for efficient electrochemical production of ammonia.

Another important aspect impacting electrocatalytic performance is structural stability and electrical tunability. Metallenes retain their metallic integrity under extreme electrochemical conditions due to strong in-plane metallic bonding, and their ultrathin shape reduces internal diffusion resistance. Furthermore, electronic tuning by alloying, defect engineering, and hybridization with conductive substrates (such as graphene or MXenes) has been extensively studied to improve catalytic efficiency. Incorporating conductive MXene substrates has been shown to significantly improve the stability, conductivity, and catalytic activity of metallene-based electrocatalysts. For instance, the NiFeP/MXene hybrid, alongside vertically interlaced nanosheet arrays, outperformed pristine NiFe-LDHs with an overpotential of 286 mV at 10 mA cm^{-2} and a Tafel slope of 35 mV dec^{-1}. This is due to strong interfacial coupling between NiFeP and $Ti_3C_2T_x$, which modulates the d-band centre and accelerates charge transfer.[144] Similarly, a Ru/MXene hybrid metallene exhibited excellent HER and OER bifunctionality, achieving a HER overpotential of 38 mV and an OER overpotential of 290 mV at 10 mA cm^{-2}, attributed to the intimate Ru–$Ti_3C_2T_x$ interface, which promotes rapid electron migration and stabilizes active Ru sites during prolonged cycling.[145] In another study, Pd nanosheets grown *in situ* on the $Ti_3C_2T_x$ MXene formed a 2D/2D heterojunction with abundant unsaturated Pd atoms and optimal interfacial electronic states, resulting in increased methanol oxidation activity with a mass activity 3.5 times greater than that of Pd/C and superior CO tolerance.[146] Overall, these findings demonstrate that MXene-metallene heterostructures combine the metallic conductivity of MXenes with the tunable surface chemistry of metallenes, resulting in strong structural integrity, rapid charge transfer, and enhanced electrocatalytic activity across a wide range of processes.

Overall, the electrocatalytic behaviour of metallenes exemplifies how metallic bonding, atomic thickness, and compositional flexibility can be used to achieve unprecedented catalytic efficiency. The strong coupling between structure and function enables precise control of catalytic parameters such as adsorption energy, electron density, and reaction kinetics. Thus, metallenes not only act as effective alternatives to noble metal catalysts but also represent a new paradigm to develop ultrathin metallic systems designed for sustainable electrochemical energy conversion technologies.

6.2. Energy storage

Metallenes have demonstrated amazing potential in energy storage due to their high electronic conductivity, enormous

surface area, and atomic-level structural tunability. These materials' ultrathin, metallic nature allows for quick charge transport and an abundance of redox-active sites, making them ideal as high-performance electrodes for batteries, supercapacitors, and hybrid energy devices. Their two-dimensional shape enables short ion diffusion paths and rapid access to the electrolyte, while metallic bonding provides mechanical stability across multiple charge–discharge cycles. Overall, the distinct physicochemical characteristics of metallenes make them a promising family of next-generation materials that bridge the gap between conventional metals and low-dimensional energy materials.

In the context of supercapacitors, metallenes offer several advantages due to their excellent electrical conductivity and structural flexibility. The abundance of exposed surface atoms promotes both fast faradaic and non-faradaic processes, which enhance double-layer and pseudocapacitive behaviour. Transition and post-transition metal-based metallenes have emerged as effective electrode materials for supercapacitors due to their large surface area, variable electronic structure, and rapid charge transfer. Traditional Ni-, Co-, and Fe-based systems exhibit good capacitance and stability, although newer post-transition counterparts, such as Ge-ene, Sn-ene, Sb-ene, and Bi-ene, perform exceptionally well. Ge-ene possesses a quantum capacitance of 60 F cm^{-2} at 0.6 V, which improves to 110.2 μF cm^{-2} with 5.6% Ti doping, resulting in increased charge storage through the formation of a double layer. Furthermore, Sn-ene exhibits high quantum capacitance at 0 volts, and co-doping enhances its electrochemical reactivity across a range of potentials. The few-layered Sb-ene reaches 1578 F g^{-1} at 14 A g^{-1} with an energy density of 20 mWh kg^{-1} at 4.8 kW kg^{-1}, while the Bi-ene/Sb-ene hybrid supercapacitor expands the voltage window to 1.5 V and ensures great stability.[147] Overall, these findings suggest that metallenes could be the next-generation supercapacitor electrodes, offering high capacitance, rapid ion transport, and long-term cycle stability.[148]

Ni-based metallenes have also demonstrated outstanding potential in supercapacitor applications due to their distinct nanosheet-assembled structures and high electrochemical activity. For instance, hierarchical Ni-MOF microflowers crafted from ultrathin nanosheets (~4.5 nm) have a high specific capacitance of 1093 F g^{-1} at 1 A g^{-1} and retain 625 F g^{-1} at 5 A g^{-1} owing to their huge surface area (52.4 m^2 g^{-1}) and open porous channels that facilitate ion diffusion. The low charge-transfer resistance (9.49 Ω) and partial transformation to $Ni(OH)_2$ during cycling improved redox activity and capacitance retention.[149] Furthermore, bimetallic and alloy metallenes, such as NiCo and FeCo, show synergistic effects in which charge redistribution between the two metals increases redox activity and electron transfer efficiency. For example, the NiCo-MOF metallene nanosheets (~3.1 nm thick) exhibited an exceptional specific capacitance of 1202 F g^{-1} at 1 A g^{-1}, retaining 76.3% after 5000 cycles with an energy density of 49.4 Wh kg^{-1} at 562.5 W kg^{-1}, ascribed to the increased ion diffusion and electron transport within its 2D porous framework, as shown in Fig. 18(a and b).[150] Similarly, the electrodeposited $FeCo_2O_4$ nanosheet metallenes exhibit a capacitance of 679 F g^{-1} at 1 A g^{-1} and 91.3% retention over 5000 cycles, owing to the linked mesopores that facilitate rapid electrolyte ion diffusion and enhanced charge storage kinetics (Fig. 18(c and d)).[151] Moreover, the hierarchical Co_3O_4@Fe-Co_2O_4 core–shell structures enhanced electrochemical activity, achieving 1649 F g^{-1} at 1 A g^{-1} and 90.6% retention after 2000 cycles, as displayed in Fig. 18(e and f). The distinct structural integration and charge redistribution of Fe, Co, and Ni centers in these ultrathin frameworks maximize redox activity and electrical conductivity, showcasing metallenes as next-generation electrode designs for high-performance supercapacitors.[152]

Building on the hybridization debate, current research shows that combining metallenes with highly conductive matrices like graphene or MXenes increases electrochemical efficiency significantly by improving charge transfer and preventing nanosheet aggregation, which can be confirmed *via* FESEM as well as HRTEM images (Fig. 18(g–j)). For instance, NiCo-MOF/$Ti_3C_2T_x$ MXene hybrid nanosheets exhibited an impressive specific capacitance of 815.2 F g^{-1} at 1 A g^{-1} and retained 82.3% of their capacitance after 10 000 cycles. The asymmetric device delivered an energy density of 39.5 Wh kg^{-1} at a power density of 562.5 W kg^{-1}. The mesoporous 2D architecture formed between NiCo and $Ti_3C_2T_x$ enabled rapid ion diffusion and good conductivity through intimate interfacial contact.[153,154] Similarly, 2D/2D MXene heterostructures, such as MXene/rGO or MXene/LDH composites, exhibit dual charge-storage behavior, combining electric double-layer and pseudocapacitive effects, which results in better energy densities (>40 Wh kg^{-1}) and exceptional cycling stability. These heterostructures benefit from interfacial synergy, in which lattice-matched contact promotes efficient ion/electron transport while impeding MXene restacking.[155] Altogether, these hybrid metallene–MXene systems show the great potential of tailored 2D-2D architectures for achieving high-rate capability, mechanical robustness, and long-term durability in next-generation supercapacitors.

Beyond capacitive storage, metallenes have been explored as active materials and conductive supports in rechargeable metal-ion batteries, including lithium-ion, sodium-ion, and zinc-ion systems. The atomically thin construction enables efficient ion diffusion and electron transport, while the metallic framework prevents structural degradation during the cycling process.[12] Among these, germanene, bismuthene, and antimonene have emerged as promising 2D anode materials for Li-ion batteries due to their distinct electrical structures and durable layered morphology. Germanene, a low-buckled honeycomb structure comparable to graphene, shows a low Li-ion diffusion barrier of 0.151 eV and a high theoretical specific capacity of 1734 mAh g^{-1}, as predicted by DFT simulations. Its open lattice framework and metallic nature enable rapid Li-ion kinetics and exceptional cycling stability while avoiding structural collapse during lithiation and delithiation.[156] Similarly, few-layered bismuthene nanosheets with a rhombohedral crystal structure

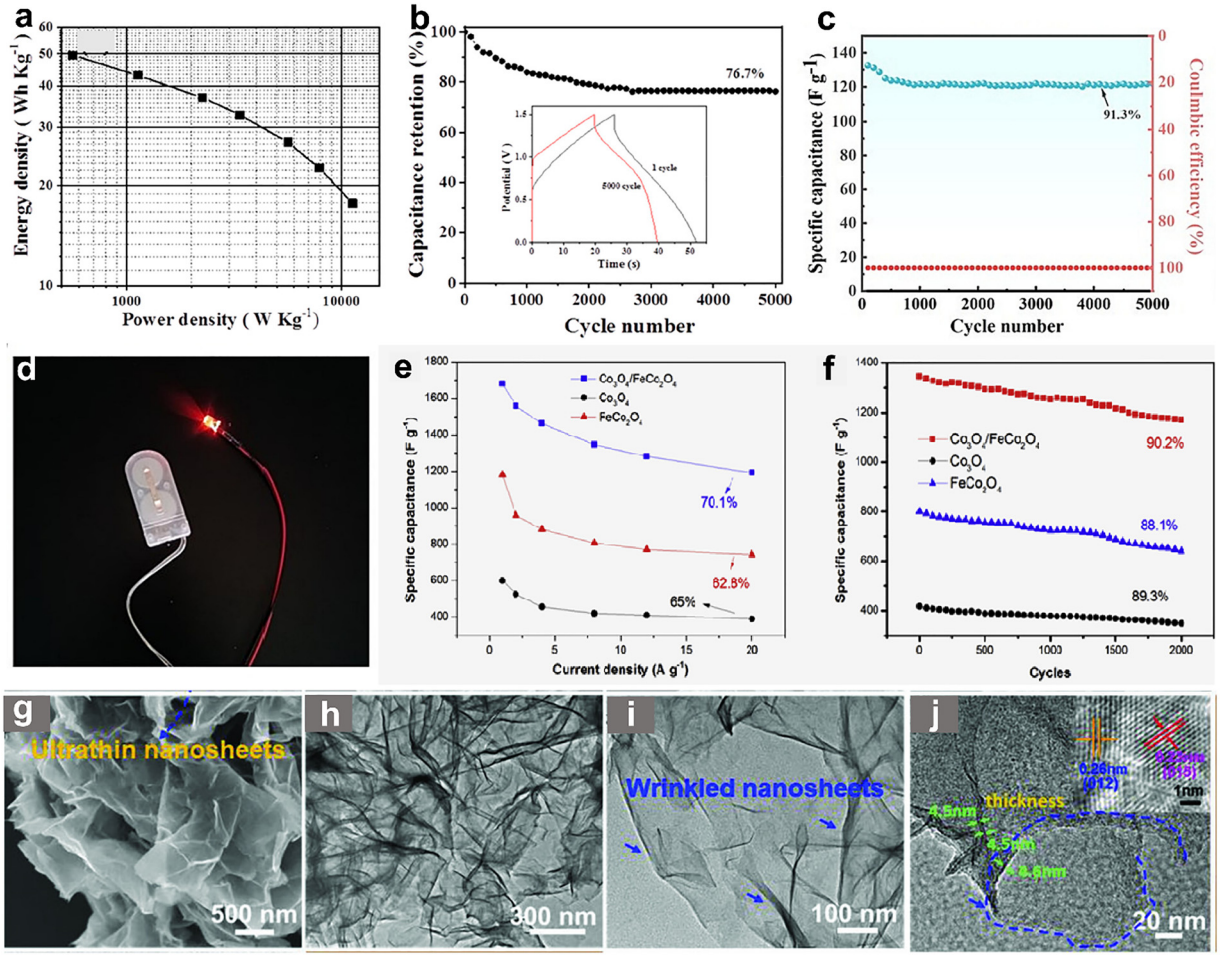

Fig. 18 Supercapacitor performances. (a) Ragone plot of the asymmetric device and (b) long-term cycling stability performances at a current density of 5 A g^{-1} over 5000 cycles. Reproduced from the ref. 150. Copyright © 2019, American Chemical Society. (c) Long cycle performance of FCS//AC ACS at a current density of 10 A g^{-1}. (d) Two asymmetric devices connected in series effectively for lighting up red LED lights. Reproduced from ref. 151 with permission from Elsevier, Copyright 2023. (e) GCD cycling test of Co_3O_4, $FeCo_2O_4$ and core–shell Co_3O_4@ $FeCo_2O_4$ electrodes and (f) specific capacitance of Co_3O_4@$FeCo_2O_4$ at various current densities. Reproduced from ref. 152 with permission from Elsevier, Copyright 2019. (g) FESEM, (h)–(j) TEM and HR-TEM images of the ultrathin NiCo-LDH-G nanosheets. Reproduced from ref. 154 with permission from Wiley, Copyright 2018.

and strong metallic bonding have shown a reversible capacity of approximately 425 mAh g^{-1} at 0.2 A g^{-1}, with an excellent 82% capacity retention after 1000 cycles. Bismuthene's puckered structure effectively buffers volumetric expansion while maintaining electronic conductivity after continuous cycling.[157] On the other hand, antimonene possesses a deformed buckling shape and high surface energy with outstanding electrochemical characteristics. It displays the reversible capacity of 660 mAh g^{-1} at 1 A g^{-1} and a 93% retention after 200 cycles. The layered structure of Sb atoms facilitates Li-ion migration channels, while the metallic framework inhibits aggregation and improves charge transfer efficiency.[158] Overall, these post-transition metallenes with their tunable atomic thickness, high surface-to-volume ratios, and intrinsic metallic character represent a new generation of ultrathin anode materials for advanced Li-ion batteries, resulting in high specific capacity, fast ion kinetics, and long-term durability.

Building on the research of metallic bonding and charge-storage mechanisms, few-layer metallenes, such as antimonene and bismuthene, show great potential as anode materials for sodium-ion batteries (SIBs) due to their structural flexibility and low ion diffusion barriers. For instance, few-layer antimonene (FLA) produced using liquid-phase exfoliation delivers reversible crystalline-phase transitions (Sb $\leftrightharpoons$ NaSb $\leftrightharpoons$ Na_3Sb), anisotropic in-plane expansion, and a low Na^+ diffusion barrier of 0.14 eV, as shown in Fig. 19(a and b). This enables a specific capacity of 642 mAh g^{-1} at 0.1C and 620 mAh g^{-1} at 0.5C with 99.7% retention after 150 cycles, resulting in 93.9% electrochemical utilization of Sb atoms (Fig. 19(c and d)).[159] Similarly, few-layer bismuthene maintains its layered structure throughout cycling and delivers a capacity of 402 mAh g^{-1} after 200 cycles at a current density of 0.2 A g^{-1}. This is attributed to its high conductivity and resilient in-plane bonding, which buffers volume changes. The buckled lattice and metallic character of metallenes are highly suited for high-capacity, long-life Na-ion storage devices, which enable rapid intercalation and alloying reactions while minimizing pulverization.[134]

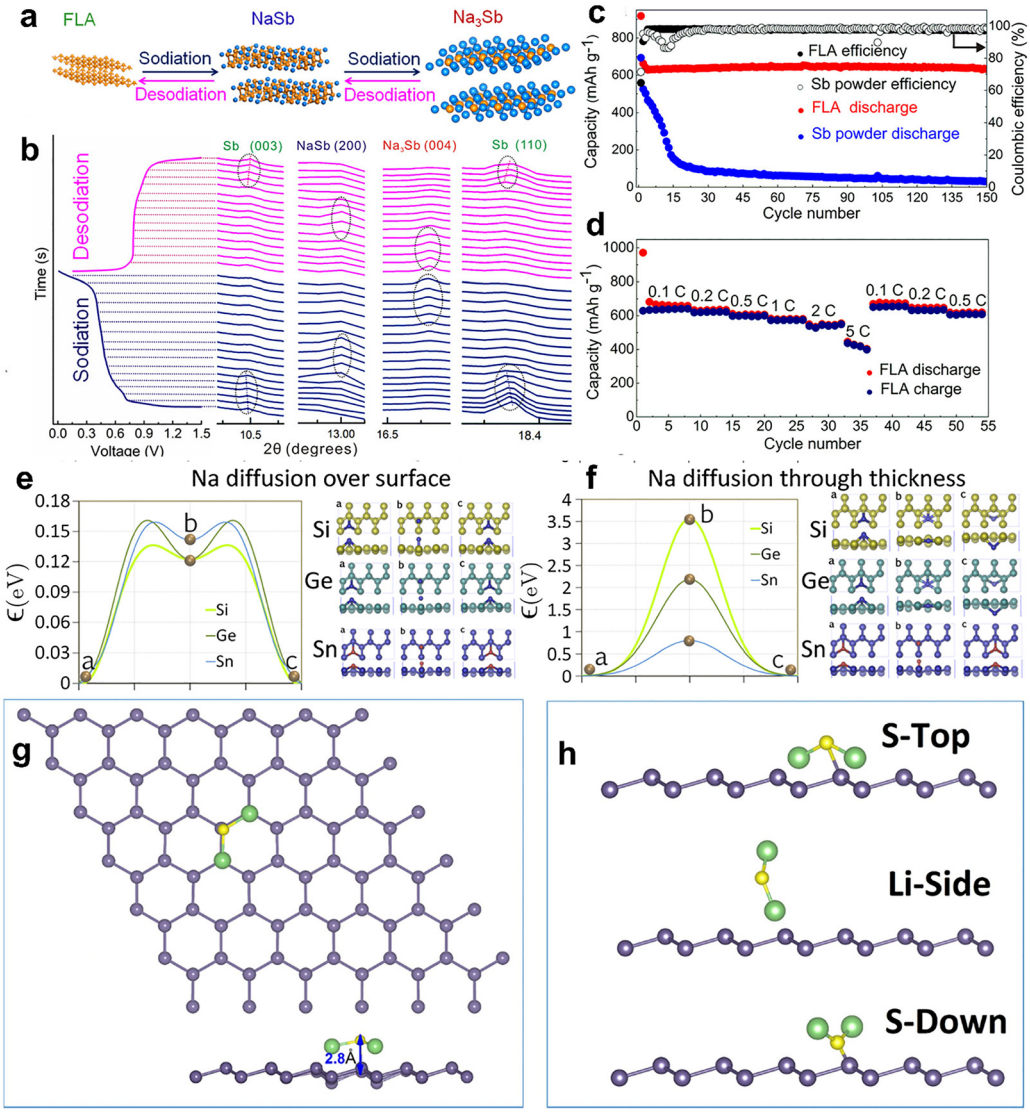

Fig. 19 Battery performances: (a) crystalline phase evolution and (b) *in situ* XRD pattern evolution of FLA anodes during the third sodiation/desodiation process. (c) Long cycling performance with coulombic efficiency of the FLA and Sb powder at 0.5C. (d) Rate capability of FLA. Reproduced from ref. 159. Copyright © 2018, American Chemical Society. (e) and (f) Diffusion energy barriers and pathways of Na adatoms in silicene, germanene and stanene. Reproduced from ref. 163 with permission from Elsevier, Copyright 2016. (g) Top and side views of ground-state configurations of GeM adsorbed. (h) Possible orientation of Li_2S with respect to GeM. Reproduced from ref. 164 with permission from Elsevier, Copyright 2021.

Building on the issues of metallic bonding and quantum confinement, 2D post-transition metallenes, such as stanene, germanene, antimonene, and bismuthene, have demonstrated substantial potential as anodes for Na-ion batteries (NIBs) due to their structural adaptability and metallic conductivity.[160] According to theoretical investigations, buckled stanene, made up of Sn atoms in a honeycomb lattice with a buckling height of ~0.85 Å and Sn–Sn bond length of 2.82 Å, is the most stable configuration for Na adsorption. Na atoms preferentially occupy hollow sites, with an adsorption energy of −0.65 eV/Na, a diffusion barrier of 0.21 eV, and an average intercalation voltage of 0.68 V, indicating rapid sodiation/desodiation kinetics and high lattice reversibility.[161,162] Similarly, germanene, with a hexagonal lattice constant of 4.01 Å and a buckling height of 0.7 Å, has a substantial Na binding energy (~1.54 eV) and a high theoretical storage capacity of 369 mAh g^{-1}, retaining metallic conductivity upon sodiation. Antimonene and bismuthene also possess layered metallic frameworks with low diffusion barriers (~0.2–0.3 eV) and high specific capacities of 650 and 402 mAh g^{-1}, respectively. This is due to their flexible 2D shape and robust in-plane bonding, thereby reducing volume expansion during cycling, as shown in Fig. 19(e and f).[163] These findings clearly reveal that the buckled and metallic structures of group IV and group V metallenes effectively balance Na-ion adsorption energy, diffusion kinetics, and mechanical stability, establishing them as highly efficient and long-lasting anode materials for next-generation Na-ion batteries.

Furthermore, beyond Li-ion and Na-ion systems, metallene architectures such as germanene and bismuthene show exceptional potential in Li–S and Mg/Zn-ion batteries, respectively,

due to their atomically thin, buckled lattice and metallic bonding nature, which enable stable ion accommodation and superior conductivity. In Li–S batteries, germanene monolayers act as highly efficient anchoring materials, immobilizing lithium polysulfides (LPSs) and efficiently minimizing the shuttle effect, which frequently causes rapid capacity loss. Furthermore, DFT calculations also show that germanene binds to LPSs with adsorption energies ranging from −1.8 to −2.6 eV, as shown in Fig. 19(g and h). This maintains metallic conductivity, allowing for rapid charge transfer across the electrode–electrolyte interface. The diffusion barriers of LPSs and Li species are extremely low, allowing for smooth ion transport and consistent redox kinetics throughout cycling. AIMD simulations indicate remarkable thermodynamic stability even at 400 K, demonstrating robustness to repeated lithiation/delithiation.[164] Similarly, in Mg/Zn-ion batteries, bismuthene monolayers have excellent divalent ion storage properties, primarily due to their strong hexagonal lattice and delocalized electronic structure. DFT and molecular dynamics simulations reveal adsorption energies of −3.38 eV (Mg) and −3.91 eV (Zn), corresponding to potential storage capacities of 2308 mAh g^{-1} for Mg and 4616 mAh g^{-1} for Zn. The associated diffusion barriers are exceptionally low (0.1 eV for Mg and 0.21 eV for Zn), and OCVs are within optimal anode potential ranges (0.01–0.03 V), ensuring rapid ion transport and steady cycling with no structural deformation or volume expansion.[165] These findings demonstrate that buckled 2D metallene frameworks not only possess great mechanical flexibility and electrical conductivity but also enable multiple-ion intercalation and surface adsorption through a combination of metallic and ionic bonding. Due to their structural plasticity and electronic adaptability, metallenes such as germanene and bismuthene serve as versatile electrode platforms capable of addressing kinetic and stability challenges in a wide range of energy storage systems, including Li–S, Mg-ion, and Zn-ion batteries.

Another important aspect is structural and electrochemical stability, which is a common issue for conventional nanometallic electrodes. Generally, metallenes have strong in-plane metallic bonding, which reduces pulverization and delamination during prolonged cycles. Encapsulation using conductive polymers or surface anchoring onto stable substrates, such as MXenes, carbon cloth, or reduced graphene oxide, has been employed to enhance mechanical integrity. These composite designs not only enhance stability but also inhibit side reactions at the electrode–electrolyte interface.[166–168] Recent advances, such as the covalently bonded MXene@Antimonene (MXene@AME) heterostructure, illustrate how metallene-based composites upsurge structural and electrochemical stability in Li-ion batteries by incorporating robust interfacial bonding and conductive frameworks, as shown in Fig. 20(a and b). This system anchors few-layer antimonene (thickness ∼2.6 nm) onto $Ti_3C_2T_x$ MXene sheets *via* Ti–O–Sb covalent bonds, substantially limiting the intrinsic ∼135% volume expansion of Sb during lithiation/delithiation. The hybrid structure retains

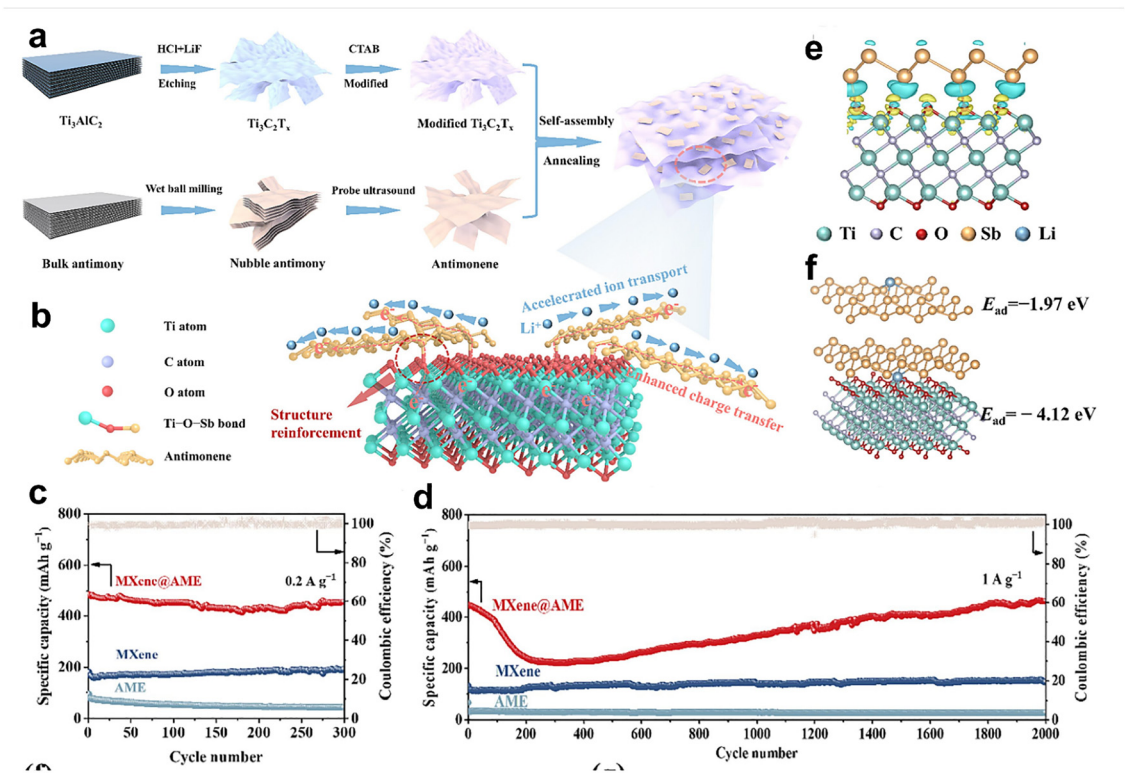

Fig. 20 (a) Synthesis route of MXene@antimonene. (b) Structural reinforcement and advantages of the MXene@antimonene heterostructure. Long cycling performances of MXene@AME, MXene and AME at the current density of (c) 0.2 Ag^{-1} and (d) 1 Ag^{-1}. (e) Charge density difference of MXene@AME. (f) Li-ion adsorption energy of AME and MXene@AME. Reproduced from ref. 169 with permission from Elsevier, Copyright 2024.

lattice integrity while introducing enlarged interlayer spacing and a hierarchical porous framework for Li^+ intercalation and electrolyte accessibility. The heterostructure exhibits a high reversible capacity of 536 mAh g^{-1} at 0.1 A g^{-1}, an outstanding rate capability of 346 mAh g^{-1} at 10 A g^{-1}, and 103.4% capacity retention after 2000 cycles, surpassing pristine antimonene and MXene equivalents, as seen in Fig. 20(c and d). Furthermore, the DFT investigation also showed a higher Li^+ adsorption energy (−4.12 eV) and a lower diffusion barrier (Fig. 20(e and f)), indicating faster charge transfer across the heterointerface.[169] These metallene-MXene structures demonstrate how strong interfacial covalent coupling and 2D metallic lattices upsurge both mechanical durability and electrochemical kinetics, opening the possibilities for next-generation high-rate, long-lasting Li-ion anodes.

Overall, the excellent combination of atomic-scale metallic bonding, structural flexibility, and customizable surface chemistry enables metallenes to be a versatile platform for various energy storage technologies. The ability to deliver high power density, rapid charge–discharge rates, and mechanical durability makes them great candidates for next-generation high-performance and energy storage systems. Continued research into heterostructured metallenes, high-entropy metallic nanosheets, and hybrid designs is projected to push the boundaries of electrochemical energy storage by combining efficiency, stability, and miniaturization on a single material platform.

7. Challenges in metallene research and applications

The key future opportunities and major challenges in metallene research and applications are illustrated in Fig. 21 and are briefly discussed below.

- The scalable and reproducible synthesis of metallenes remains challenging because precise control over thickness, lateral dimensions, crystallinity, and compositional uniformity is still limited.
- Current preparation methods often exhibit low yield and batch variability, necessitating the development of cost-effective, environmentally sustainable, and industrially viable production strategies.
- The long-term electrochemical stability of metallenes is restricted by oxidation, aggregation, dissolution, and structural reconstruction under harsh reaction conditions.
- The dynamic evolution of surface structures during electrocatalytic reactions complicates the identification of true active sites and the establishment of reliable structure–activity relationships.
- A comprehensive mechanistic understanding requires advanced *in situ* and *operando* characterization combined with accurate theoretical modeling to bridge the gap between experimental observations and predictions.
- Practical device integration is hindered by issues related to electrode fabrication, interfacial compatibility, mechanical robustness, and the high cost of noble-metal-based systems.

8. Conclusions and prospects

Metallenes are a rapidly developing family of two-dimensional metallic materials with exceptional catalytic and electrochemical capabilities due to their atomically thin structure, significant surface exposure, and distinct electronic configuration. They are distinguished from bulk metals and ordinary nanostructures by their unusual coordination environments, tunable lattice distortions, and altered electronic states, which enable

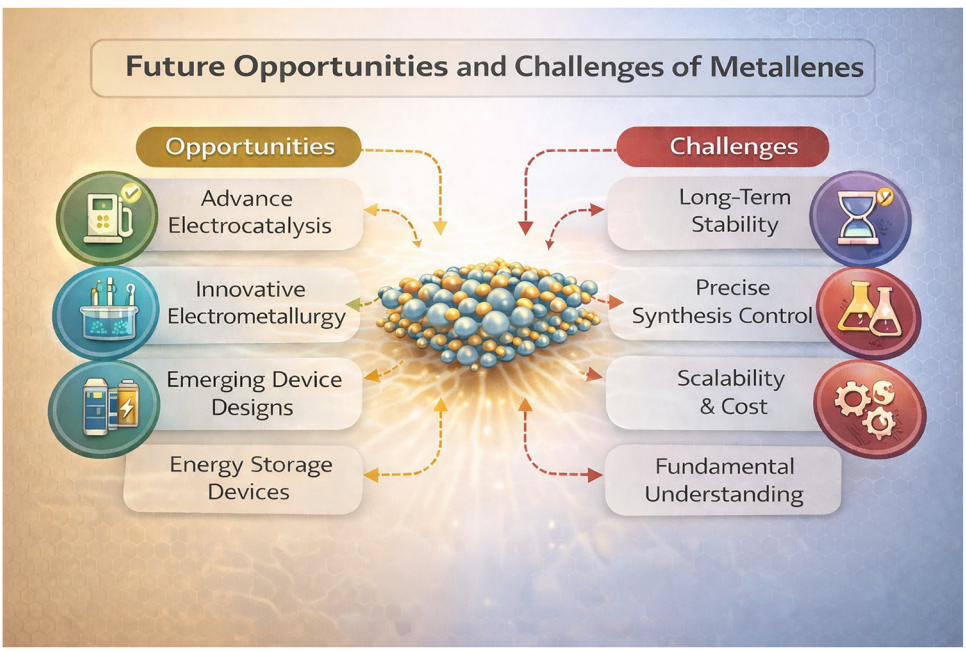

Fig. 21 Overview of the key future opportunities and major challenges in metallene research and applications.

remarkable activity in electrocatalytic reactions such as the HER, OER, ORR, and CO_2RR. Additionally, metallenes have strong interfacial interactions with electrolytes, fast charge-transfer kinetics, and good conductivity, making them attractive and desirable alternatives for high-performance energy storage systems, including metal–air batteries, supercapacitors, and sophisticated hybrid devices. The structural diversity and functional tunability of metallene systems have been significantly enhanced by ongoing advancements in synthetic techniques, from wet-chemical and electrochemical pathways to template-assisted and interface-driven growth, indicating their wide potential for next-generation sustainable energy technologies. In this context, the integration of advanced characterization techniques, predictive theoretical modelling, and data-driven materials design is expected to accelerate rational optimization and practical implementation. With sustained interdisciplinary efforts spanning synthesis, mechanistic insight, and device engineering, metallenes are poised to emerge as a foundational platform for efficient, durable, and economically viable energy conversion and storage techniques.

Author contributions

SES and ACR: literature search, data collection, and writing – original draft; JHO: writing – reviewing and editing; SHL: funding acquisition, resources, reviewing and editing; SA: conceptualization, resources, supervision, validation, reviewing and editing.

Conflicts of interest

There are no conflicts to declare.

Data availability

No primary research results, software, or code have been included, and no new data were generated or analyzed in this review article. All figures and tables are derived from previously published sources, which are cited appropriately in the text. Selected schematic illustrations (Fig. 4, 9–15, and 21), and the Graphical abstract were generated using AI-assisted tools and subsequently reviewed and refined by the authors. These figures are intended solely for conceptual visualization and do not represent original experimental data or results.

Acknowledgements

The authors gratefully acknowledge the financial support from the National Research Foundation of Korea (NRF) under the Brain Pool Program (Grant No. RS-2024-00446898) and additional support through Grant No. RS-2023-00213746 and RS-2025-25400034. Furthermore, the authors acknowledge the Regional Innovation System & Education (RISE) program through the Chungbuk Regional Innovation System & Education Center, funded by the Ministry of Education (MoE) and Chungcheongbuk-do, Republic of Korea (Grant No. 2025-RISE-11-004-03).

References

1 F. Ren, Z. Han, L. Zhu, Z. Lei, G. Shi and Z. Li, *et al.*, Metallene: Ångström-Scale 2D Metals, *Adv. Mater.*, 2025, **306**, 1–39.
2 H. Q. Ta, R. G. Mendes, Y. Liu, X. Yang, J. Luo and A. Bachmatiuk, *et al.*, In Situ Fabrication of Freestanding Single-Atom-Thick 2D Metal/Metallene and 2D Metal/Metallene Oxide Membranes: Recent Developments, *Adv. Sci.*, 2021, **8**(20), 1–36.
3 A. C. Radjendirane, S. Ramakrishnan, S. P. Rajendra, K. Vediappan, I. In and S. J. Lee, *et al.*, Engineering Ti-MXene integrated interpenetrating polymer network based hybrid hydrogel electrolytes for high- performance flexible zinc-ion batteries, *J. Power Sources*, 2025, **652**(237660), 1–7.
4 S. Kartigueyane, S. P. Arunachala Kumar, M. S. Alsalhi, S. P. Rajendra, I. In and S. J. Lee, *et al.*, Electrocatalytic Activity of Multifunctional Mn-Doped SrFeO 3- δ/Ti- MXene Nanohybrid for Efficient Overall Water Splitting, *Appl. Energy Mater.*, 2025, **8**(8), 5004–5016.
5 C. Tang and S. Z. Qiao, 2D Atomically Thin Electrocatalysts: From Graphene to Metallene, *Matter*, 2019, **1**(6), 1454–1455.
6 K. R. Abidi, M. Bagheri, S. Singh and P. Koskinen, Atomically thin metallenes at the edge, *2D Mater.*, 2025, **12**(2), 23–26.
7 K. R. Abidi and P. Koskinen, Electronic and structural properties of atomically thin metallenes, *Electron Struct.*, 2025, **7**(1), 23–26.
8 M. K. Kabiraz, H. Wahidah, J. W. Hong and S. il Choi, Platinum Metallenes: Advanced Electrocatalysts for Sustainable Energy Conflict of Interest, *Small*, 2025, **21**(27), 1–16.
9 M. A. B. Kabatas, A Comprehensive Review on Electrocatalytic Applications of 2D Metallenes, *Nanomaterials*, 2023, **13**(22), 1–2.
10 Y. Anil, R. Mohan, N. Kalla, R. Khan, A. G. Al-sehemi and A. Ghosh, Double-transition metal MXenes for energy storage and conversion applications, *J. Power Sources*, 2026, **665**, 1–6.
11 T. Ramachandran, M. P. Pachamuthu, R. K. Raji, F. R. Maria and S. Raj, A layered Fe – SnO 2/MXene nanohybrid with 1225. 6 F g^{-1} capacitance and long-term cycle durability, *Mater. Chem. Phys.*, 2026, **350**, 1–5.
12 Y. Liu, K. Dinh, Z. Dai and Y. Q. Fei, Metallenes: Recent Advances and Opportunities in Energy Storage and Conversion Applications, *ACS Mater. Lett.*, 2020, **93**, 1–9.
13 B. Jiang, Y. Guo, F. Sun, S. Wang, Y. Kang and X. Xu, *et al.*, Nanoarchitectonics of Metallene Materials for Electrocatalysis, *ACS Nano*, 2023, **17**(14), 13017–13043.
14 M. Xie, S. Tang, B. Zhang and G. Yu, Metallene-related materials for electrocatalysis and energy conversion, *Mater. Horiz.*, 2023, **2**, 1–37.

15 C. Lu, R. Li, Z. Miao, F. Wang and Z. Zha, Emerging metallenes: synthesis strategies, biological effects and biomedical applications, *Chem. Soc. Rev.*, 2023, **8**, 1–12.
16 A. C. Radjendiran, M. F. Sha, B. Balan, S. Ramakrishnan, K. Vediappan, P. S. Rajendra and A. S. Mohamad, 3D-Polyacrylamide/Ti-MXene: A Newer Hybrid Hydrogel Electrolyte Featuring High Mechanical Strength and Durability for Flexible Aqueous Zinc-Ion Batteries, *ACS Appl. Energy Mater.*, 2024, **7**(11), 4745–4760.
17 A. C. Radjendirane, S. Ramasamy, S. P. Rajendra, I. In, S. J. Lee and S. Angaiah, Mechanically endurable Ti 3 C 2 T x MXene incorporated P (AM-AA) hybrid hydrogel electrolyte with enhanced Zn 2 + conductivity for flexible zinc-ion batteries, *Electrochim. Acta*, 2025, **531**(146368), 1–9.
18 B. Kirubasankar, B. Balan, C. Yan and S. Angaiah, Recent Progress in Graphene-Based Microsupercapacitors, *Energy Technol.*, 2021, **9**(5), 1–25.
19 P. Prabhu and J. Lee, Metallenes as functional materials in electrocatalysis Abstract, *Chem. Soc. Rev.*, 2021, **12**, 1–5.
20 O. Bubnova, A new metallene arrival, *Nat. Nanotechnol.*, 2018, **13**(171), 24–26.
21 F. Wang, Z. Wang, T. A. Shifa, Y. Wen, F. Wang and X. Zhan, *et al.*, Two-Dimensional Non-Layered Materials: Synthesis, Properties and Applications, *Adv. Funct. Mater.*, 2017, **27**(19), 1–15.
22 W. Tao, N. Kong, X. Ji, Y. Zhang, A. Sharma and J. Ouyang, *et al.*, Emerging two-dimensional monoelemental materials (Xenes) for biomedical applications, *Chem. Soc. Rev.*, 2019, **11**, 1–5.
23 M. Pumera and Z. Sofer, 2D Monoelemental Arsenene, Antimonene, and Bismuthene: Beyond Black Phosphorus, *Adv. Mater.*, 2017, **29**(21), 28185366.
24 Y. Wang, M. Chen and F. Zhou, High tensile ductility in a nanostructured metal, *Nature*, 2002, **419**, 912–915.
25 C. Wei and C. Zhu, Cryogenic Exfoliation of Non-layered Magnesium into Two-Dimensional Crystals, *Angew. Chem., Int. Ed.*, 2019, **58**(26), 8814–8818.
26 A. Allotropes, G. Wang, R. Pandey and S. P. Karna, Atomically Thin Group V Elemental Films: Theoretical Investigations of, *ACS Appl. Mater. Interfaces*, 2015, **7**(21), 11490–11496.
27 E. Aktürk, O. Ü. Aktürk and S. Ciraci, Single and bilayer bismuthene: Stability at high temperature and mechanical and electronic properties, *Phys. Rev. B*, 2016, **94**(014115), 23–25.
28 A. Acun, L. Zhang, P. Bampoulis, M. Farmanbar, A. V. Houselt and A. N. Rudenko, *et al.*, Germanene: the germanium analogue of graphene, *J. Phys.: Condens. Matter*, 2015, **27**(44), 25–28.
29 J. Deng, B. Xia, X. Ma, H. Chen, H. Shan and X. Zhai, Epitaxial growth of ultraflat stanene with topological band inversion, *Nat. Mater.*, 2018, **17**(12), 1081–1086.
30 X. Huang, S. Li, Y. Huang, S. Wu, X. Zhou and S. Li, *et al.*, Synthesis of hexagonal close-packed gold nanostructures, *Nat. Commun.*, 2011, **2**(292), 1–21.
31 Z. Fan, M. Bosman, X. Huang, D. Huang, Y. Yu and K. P. Ong, *et al.*, Stabilization of 4H hexagonal phase in gold nanoribbons, *Nat. Commun.*, 2015, **6**(7684), 1–28.
32 X. Huang, H. Li, S. Li, S. Wu and F. Boey, Synthesis of Gold Square-like Plates from Ultrathin Gold Square Sheets, *Angew. Chem., Int. Ed.*, 2011, **50**(51), 12245–12248.
33 Q. Yun, Q. Lu, C. Li, B. Chen, Q. Zhang and Q. He, *et al.*, Synthesis of PdM (M = Zn, Cd, ZnCd) Nanosheets with an Unconventional Face-Centered Tetragonal Phase as Highly Efficient Electrocatalysts for Ethanol Oxidation, *ACS Nano*, 2019, **13**(12), 14329–14336.
34 L. Wang, Y. Zhu, J. Q. Wang, F. Liu, J. Huang and X. Meng, Two-dimensional gold nanostructures with high activity for selective oxidation of carbon – hydrogen bonds, *Nat. Commun.*, 2015, **6**(6957), 1–25.
35 Y. Feng, B. Huang, C. Yang, Q. Shao and X. Huang, Platinum Porous Nanosheets with High Surface Distortion and Pt Utilization for Enhanced Oxygen Reduction Catalysis, *Adv. Funct. Mater.*, 2019, **29**(45), 1–9.
36 Q. Luo, C. Sun, J. Zhao and C. Q. Juan, Highly Efficient SnIn4S8@ZnO Z-Scheme Heterojunction Photocatalyst for Methylene Blue Photodegradation, *Materials*, 2023, **16**(19), 1–8.
37 M. Andrea, G. Abellán and M. A. Lucherelli, Chemistry of two-dimensional pnictogens: advanced applications, *Chem. Commun.*, 2023, **59**(43), 1–10.
38 C. C. Mayorga-martinez, R. Gusmão, P. Zden and P. M. Pumera, Pnictogen-Based Enzymatic Phenol Biosensors: Phosphorene, Arsenene, Antimonene, and Bismuthene, *Angew. Chem., Int. Ed.*, 2018, **58**(1), 134–138.
39 C. Li, F. Gao, Y. Ren, B. Li, L. Li., Z. Lu, X. Yang, X. Zhang and X. Yu, PtPdMo Nanosheets with Controllable Synthesis for Enhanced Oxygen Reduction Reactions, *ACS Appl. Nano Mater.*, 2022, **5**(1), 1192–1199.
40 Y. Leng, Y. Wang, X. Li, T. Liu and S. Takahashhi, Controlled synthesis of triangular and hexagonal Ni nanosheets and their size-dependent properties, *Nanotechnology*, 2006, **17**(19), 23–26.
41 J. Zhao, Q. Deng, A. Bachmatiuk, G. Sandeep, A. Popov and J. Eckert, Free-Standing Single-Atom-Thick Iron Membranes Suspended in Graphene Pores, *Science*, 2014, **343**(6176), 1228–1232.
42 K. A. Willets, K. A. Willets and C. M. Marian, Localized Surface Plasmon Resonance Spectroscopy and Sensing, *Annu. Rev. Phys. Chem.*, 2007, **0**(30), 1–2.
43 K. Nisi, S. Subramanian, W. He, K. A. Ulman, H. El-sherif and F. Sigger, *et al.*, Light–Matter Interaction in Quantum Confined 2D Polar Metals, *Adv. Funct. Mater.*, 2021, **31**(4), 1–30.
44 X. Huang, S. Tang, X. Mu, Y. Dai, G. Chen and Z. Zhou, Freestanding palladium nanosheets with plasmonic and catalytic properties, *Nat. Nanotechnol.*, 2011, **6**(1), 28–32.
45 Y. Chen, Z. Fan, Z. Zhang, W. Niu, C. Li and N. Yang, *et al.*, Two-Dimensional Metal Nanomaterials: Synthesis, Properties, and Applications, *Chem. Rev.*, 2018, **118**(13), 6409–6455.
46 S. He, G. Zhu, Z. Sun, J. Wang, P. Hui and P. Zhao, 2D AuPd alloy nanosheets: one-step synthesis as imaging-guided photonic nano- antibiotics, *Nanoscale Adv.*, 2020, **2**, 3550–3560.

47 M. F. Tsai, S. H. Chang, F. Y. Cheng, V. Shanmugam, Y. S. Cheng, C. H. Su and C. S. Yeh, Au nanorod design as light-absorber in the first and second biological near-infrared windows for *in vivo* photothermal therapy, *ACS Nano*, 2013, **7**(6), 5330–5342.
48 Y. Zhang, Q. Shen, Q. Li, P. He, J. Li and F. Huang, *et al.*, Ultrathin Two-Dimensional Plasmonic PtAg Nanosheets for Broadband Phototheranostics in Both NIR-I and NIR-II Biowindows, *Adv. Sci.*, 2021, **8**(17), 1–16.
49 N. Hussain, T. Liang, Q. Zhang, T. Anwar, Y. Huang and J. Lang, *et al.*, Ultrathin Bi Nanosheets with Superior Photoluminescence, *Small*, 2017, **13**(36), 1–10.
50 F. Zhang, J. He, Y. Xiang, K. Zheng, B. Xue and S. Ye, *et al.*, Semimetal–Semiconductor Transitions for Monolayer Antimonene Nanosheets and Their Application in Perovskite Solar Cells, *Adv. Mater.*, 2018, **30**(38), 1–10.
51 Y. Liu, Y. Xiao, M. Yu, Y. Cao, Y. Zhang and T. Zhe, *et al.*, Antimonene Quantum Dots as an Emerging Fluorescent Nanoprobe for the pH- Mediated, *Small*, 2020, **16**(42), 1–8.
52 Z. L. Lei and B. Guo, 2D Material-Based Optical Biosensor: Status and Prospect, *Adv. Sci.*, 2022, **9**(4), 1–90.
53 R. Duan, X. Lou and F. Xia, The development of nanostructure assisted isothermal amplification in biosensors, *Chem. Soc. Rev.*, 2015, **6**, 1–45.
54 Y. Xu, B. Wang, R. Kaur, M. B. Minameyer, M. Bothe and P. T. Drewello, *et al.*, A Supramolecular [10]CPP Junction Enables Efficient Electron Transfer in Modular Porphyrin – [10]CPP ⊃ Fullerene Complexes, *Angew. Chem., Int. Ed.*, 2018, **57**(36), 11549–11553.
55 X. Duan, Z. Liu, Z. Xie, A. K. Tareen, K. Khan, B. Zhang and H. Zhang, Emerging monoelemental 2D materials (Xenes) for biosenso applications, *Nano Res.*, 2023, **16**(5), 7030–7052.
56 H. Wang, L. Yang, Z. Song and N. Hui, Glycyrrhiza polysaccharide doped the conducting polymer PEDOT hybrid-modified biosensors for the ultrasensitive detection of microRNA, *Anal. Chim. Acta*, 2020, **1139**, 155–163.
57 T. Ramachandran, R. Mohan, N. Kalla, R. Khan, Y. A. Kumar and A. K. Yadav, *et al.*, Heteroatom doping of MXenes in supercapacitor applications, *J. Power*, 2026, **664**, 1–6.
58 Y. Ma, B. Li and S. Yang, Ultrathin two-dimensional metallic nanomaterials Yang, *Mater. Chem. Front.*, 2018, **2**, 456–467.
59 H. Zhou, Z. Li, Z. Wang, T. Wang, L. Xu and Y. He, *et al.*, Hydrogenation of quinolines using a recyclable phosphine-free chiral cationic ruthenium catalyst: enhancement of catalyst stability and selectivity in an ionic liquid, *Angew. Chem., Int. Ed.*, 2008, **47**(44), 8464–8467.
60 N. Abid, A. M. Khan, S. Shujait, K. Chaudhary and M. Ikram, Synthesis of nanomaterials using various top-down and bottom-up approaches, influencing factors, advantages, and disadvantages: A review, *Adv. Colloid Interface Sci.*, 2022, **300**(102597).
61 P. Gao, Y. Xiao, L. Li, W. Li and W. Tao, Biomedical applications of 2D monoelemental materials formed by group VA and VIA: a concise review, *J. Nanobiotechnol.*, 2021, **19**(96), 1–61.
62 X. Zhao, L. Dai, Q. Qin, F. Pei, C. Hu and N. Zheng, Self-Supported 3D PdCu Alloy Nanosheets as a Bifunctional Catalyst for Electrochemical Reforming of Ethanol, *Small*, 2017, **13**(12), 1–9.
63 H. Liu, A. T. Neal, Z. Zhu, Z. Luo, X. Xu and D. Tomanek, *et al.*, Phosphorene: An Unexplored 2D Semiconductor with a High Hole Mobility, *ACS Nano*, 2014, **8**(4), 4033–4041.
64 P. Ares, F. Aguilar-galindo, D. Rodríguez-san-miguel and D. A. Aldave, Mechanical Isolation of Highly Stable Antimonene under Ambient Conditions, *Adv. Funct. Mater.*, 2016, **28**(30), 6332–6336.
65 A. Castellanos-gomez, L. Vicarelli, E. Prada, J. O. Island, S. I. Blanter and D. J. Groenendijk, *et al.*, Isolation and characterization of few-layer black phosphorus Code, Data and Media Associated with this Article, *2D Mater.*, 2014, **1**(2), 23–26.
66 E. b Flint and K. S. Suslick, The Temperature of Cavitation, *Science*, 1991, **253**(5026), 1–6.
67 W. Lu, B. Birmingham, D. V. Voronine, D. Stolpman, S. Ambardar and D. A. Erdogan, *et al.*, From Aluminum Foil to Two-Dimensional Nanocrystals Using Ultrasonic Exfoliation, *J. Phys. Chem.*, 2021, **125**, 7746–7755.
68 T. P. Yadav, C. F. Woellner, T. Sharifi, S. K. Sinha, L. Qu and A. Apte, *et al.*, Extraction of Two-Dimensional Aluminum Alloys from Decagonal, *ACS Nano*, 2020, **14**(6), 7435–7443.
69 C. Gibaja, D. Rodriguez-san-miguel and P. Ares, Few-Layer Antimonene by Liquid-Phase Exfoliation, *Angew. Chem., Int. Ed.*, 2016, **55**(46), 14345–14349.
70 R. Gusmão, Z. Sofer and M. Pumera, Black Phosphorus Rediscovered: From Bulk Material to Monolayers, *Angew. Chem., Int. Ed.*, 2017, **56**(28), 8052–8072.
71 C. Xing, W. Huang, Z. Xie, J. Zhao, D. Ma, T. Fan, W. Liang, Y. Ge, B. Dong, J. Li and H. Zhang, Ultrasmall bismuth quantum dots: facile liquid-phase exfoliation, characterization, and application in high-performance UV – Vis photodetector, *ACS Photonics*, 2018, **5**(2), 621–629.
72 Z. Huang, H. Hou, Y. Zhang, C. Wang, X. Qiu and X. Ji, Layer-Tunable Phosphorene Modulated by the Cation Insertion Rate as a Sodium-Storage Anode, *Adv. Mater.*, 2017, **29**(34), 1–10.
73 D. Wu, X. Shen, J. Liu, C. Wang, Y. Liang and X. Fu, *et al.*, Electrochemical exfoliation from an industrial ingot: ultrathin metallic bismuth nanosheets for excellent CO capture and electrocatalytic conversion, *Nanoscale*, 2019, **45**, 5–9.
74 A. M. Marzo, R. Gusmão, Z. Sofer and M. Pumera, Towards Antimonene and 2D Antimony Telluride through Electrochemical Exfoliation, *Chem. Eur. J.*, 2020, **26**(29), 6583–6590.
75 H. S. Tsai, C. W. Chen, C. H. Hsiao, H. Ouyang and J. H. Liang, The advent of multilayer antimonene nanoribbons with room temperature orange light emission, *Chem. Commun.*, 2016, **54**, 1–5.
76 V. Kochat, A. Samanta, Y. Zhang, S. Bhowmick, P. Manimunda, S. A. Asif, A. S. Stender, R. Vajtai, A. K. Singh, C. S. Tiwary and P. M. Ajayan, Atomically thin

gallium layers from solid-melt exfoliation, *Mater. Sci.*, 2018, **4**(3), 1–18.
77 X. Wang, C. Wang, C. Chen, H. Duan and K. Du, Free-standing Monatomic Thick Two-dimensional Gold, *Nano Lett.*, 2019, **19**(7), 4560–4566.
78 J. Ma, J. Gu, B. Li and S. Yang, Facile fabrication of 2D stanene nanosheets via a dealloying strategy for potassium storage, *Chem. Commun.*, 2019, **27**, 5–9.
79 J. R. Arthur, Molecular beam epitaxy, *Surf. Sci.*, 2002, **500**(1–3), 189–217.
80 A. Y. Cho and J. R. Arthur, Molecular beam epitaxy Recommended articles, *Prog. Solid State Chem.*, 1975, **6786**(75), 23–26.
81 T. Niu, Q. Meng, D. Zhou, N. Si, S. Zhai and X. Hao, *et al.*, Large-Scale Synthesis of Strain-Tunable Semiconducting Antimonene on Copper Oxide, *Adv. Mater.*, 2020, **32**(4), 1–10.
82 X. Wu, Y. Shao, H. Liu, Z. Feng, Y. L. Wang and J. T. Sun, *et al.*, Epitaxial Growth and Air-Stability of Monolayer Antimonene on PdTe 2, *Adv. Mater.*, 2017, **29**(11), 28028843.
83 M. Fortin-Deschênes, O. Waller, T. O. Mentes, A. Locatelli, S. Mukherjee, F. Genuzio, P. L. Levesque, A. Hebert, R. Martel and O. Moutanabbir, Synthesis of Antimonene on Germanium, *Nano Lett.*, 2017, **9**(17), 4970–4975.
84 E. S. Walker, S. R. Na, D. Jung, S. D. March, J. S. Kim, T. Trivedi, W. Li, L. Tao, M. L. Lee, K. M. Liechti and D. Akinwande, Large-Area Dry Transfer of Single-Crystalline Epitaxial Bismuth Thin Films, *Nano Lett.*, 2016, **16**(11), 6931–6938.
85 Y. Deng, W. Chen, B. Li and C. Wang, Physical vapor deposition technology for coated cutting tools: A review, *Ceram. Int.*, 2020, **46**(44), 18373–18390.
86 R. Platz and S. Wagner, Intrinsic microcrystalline silicon by plasma-enhanced chemical vapor deposition from dichlorosilane, *Appl. Phys. Lett.*, 1998, **73**, 1236–1238.
87 J. Yu, J. Li, W. Zhang and H. Chang, Synthesis of high quality two-dimensional materials via chemical vapor deposition, *Chem. Sci.*, 2015, **6**, 6705–6716.
88 H. S. Tsai, Y. Z. Chen, H. Medina, T. Y. Su, T. S. Chou, Y. H. Chen, Y. L. Chueh and J. H. Liang, Direct formation of large-scale multi-layered germanene on Si substrate, *Phys. Chem. Chem. Phys.*, 2015, **33**, 1–5.
89 S. Kuriakose, S. K. Jain, S. A. Tawfik, M. J. S. Spencer, B. J. Murdoch and M. Singh, *et al.*, Monocrystalline Antimonene Nanosheets via Physical Vapor Deposition Sruthi, *Adv. Mater. Interfaces*, 2020, **7**(24), 1–10.
90 O. A. Options, High-Yield Seedless Synthesis of Triangular Gold Nanoplates through Oxidative Etching, *Nano Lett.*, 2014, **14**(12), 7201–7206.
91 Q. Yang, L. Shi, B. Yu, J. Xu, C. Wei and Y. Wang, *et al.*, Facile synthesis of ultrathin Pt–Pd nanosheets for enhanced formic acid oxidation and oxygen reduction reaction, *J. Mater. Chem. A*, 2019, **32**, 5–9.
92 Z. Fan, X. Huang, Y. Han, M. Bosman, Q. Wang and Y. Zhu, *et al.*, Surface modification-induced phase transformation of hexagonal close-packed gold square sheets, *Nat. Commun.*, 2015, **6**(6571), 1–28.
93 Z. Fan, Y. Zhu, Q. Wang and Y. Huang, Synthesis of Ultrathin Face-Centered-Cubic Au@Pt and Au@Pd Core–Shell Nanoplates from Hexagonal-Close-Packed Au Square Sheets, *Angew. Chem.*, 2015, **127**(19), 5764–5768.
94 P. D. A. Rabenau, First. The Role of Hydrothermal Synthesis in Preparative Chemistry, *Angew. Chem., Int. Ed. Engl.*, 1985, **24**(12), 1026–1040.
95 J. Lai, W. Niu, R. Luque and G. Xu, Solvothermal synthesis of metal nanocrystals and their applications, *Nano Today*, 2015, **10**(2), 240–267.
96 H. Duan, N. Yan and R. Yu, Chang C ran, Zhou G, Hu H shi, *et al.* Ultrathin rhodium nanosheets, *Nat. Commun.*, 2014, **5**(3093), 1–26.
97 J. Yang, L. Lu, H. Wang, W. Shi and H. Zhang, Glycyl Glycine Templating Synthesis of Single-Crystal Silver, *Cryst. Growth Des.*, 2006, **6**(9), 2155–2158.
98 J. Zhang, S. Ye, Y. Sun, F. Zhou, J. Song and J. Qu, Soft-template assisted synthesis of hexagonal antimonene and bismuthene in colloidal solutions, *Nanoscale*, 2020, **40**, 23–27.
99 D. Xu, Y. Liu, S. Zhao, Y. Lu, M. Han and J. Bao, Novel surfactant-directed synthesis of ultra-thin palladium nanosheets as efficient electrocatalysts for glycerol oxidation, *Chem. Commun.*, 2017, **10**, 1–5.
100 K. V. V. Chandra, D. Mani, T. Ramachandran, Y. Anil and A. Ghosh, A new era in energy storage: In Situ and Operando characterization of 2D materials-based devices, *Mater. Chem. Phys.*, 2026, **348**, 1–8.
101 R. F. Egerton, Radiation damage to organic and inorganic specimens in the TEM, *Micron*, 2019, **119**(30684768), 72–87.
102 S. Yang, Y. Gong, P. Manchanda, Y. Zhang, G. Ye and S. Chen, Rhenium-Doped and Stabilized MoS Atomic Layers with Basal-Plane Catalytic Activity, *Adv. Mater.*, 2018, **30**(51), 1–8.
103 A. C. Ferrari and D. M. Basko, Raman spectroscopy as a versatile tool for studying the properties of graphene Andrea, *Nat. Nanotechnol.*, 2013, **8**, 235–246.
104 J. Timoshenko, Z. Duan, G. Henkelman and R. M. F. A. I. Crooks, Solving the Structure and Dynamics of Metal Nanoparticles by Combining X- Ray Absorption Fine Structure Spectroscopy and Atomistic Structure Simulations, *Annu. Rev. Phys. Chem.*, 2019, **12**, 1–28.
105 B. Ravel and M. A. Newville, Athena, Artemis, Athena, Artemis, Hephaestus: data analysis for X-ray absorption spectroscopy using using IFEFFIT, *J. Synchrotron Radiat.*, 2005, **12**, 537–541.
106 L. Bijelić, F. Ruiz-Zepeda and N. Hodnik, The role of high-resolution transmission electron microscopy and aberration corrected scanning transmission electron microscopy in unraveling the structure–property relationships of Pt-based fuel cells electrocatalysts, *Inorg. Chem. Front.*, 2024, **11**, 323–341.
107 P. D. Nellist, Scanning Transmission Electron Microscopy, *Springer Handbook of Microscopy*, 2019, pp. 49–99.
108 G. Greczynski and L. Hultman, X-ray photoelectron spectroscopy: Towards reliable binding energy referencing, *Prog. Mater. Sci.*, 2020, **107**(100591), 1–91.

109 E. C. Le Ru and P. G. Etchegoin, Single-Molecule Surface-Enhanced Raman Spectroscopy, *Annu. Rev. Phys. Chem.*, 2011, **63**(1), 65–87.
110 S. R. Khan, B. Sharma and R. Bhatia, Inductively Coupled Plasma Optical Emission Spectrometry (ICP-OES): a Powerful Analytical Technique for Elemental Analysis, *Food Anal. Methods*, 2021, **15**, 668–688.
111 K. Kaja, P. Regreny and N. Chauvin, Atomic force microscopy as a multimetrological platform for energy devices, *Nanoscale*, 2025, **14**, 1–17.
112 R. T. Vang, J. V. Lauritsen and F. Besenbacher, Scanning tunneling microscopy as a tool to study catalytically relevant model systems, *Chem. Soc. Rev.*, 2008, **10**, 1–5.
113 J. A. Schuller, E. S. Barnard, W. Cai, Y. C. Jun, J. S. White and L. Mark, Plasmonics for extreme light concentration and manipulation, *Nat. Mater.*, 2010, **9**, 193–204.
114 U. Shukla and S. Bari, Study on the Photoluminescence, *J. Pure Appl. Ind. Phys.*, 2018, **8**(5), 1–6.
115 J. Wang, J. Dziadkowiec, Y. Liu, W. Jiang, Y. Zheng and P. Peng, Combining atomic force microscopy and nanoindentation helps characterizing in situ mechanical properties of organic matter in shale, *Int. J. Coal Geol.*, 2024, **281**, 104406.
116 M. E. Brown and P. K. Gallagher, *Handbook of Therrmal Analysis*, Kluwer, 2003, p. 36.
117 N. Argaman and G. Makov, Density functional theory: An introduction, *Am. J. Phys.*, 2000, **68**, 69–79.
118 A. A. Bliznyuk and J. E. Gready, Combining docking and molecular dynamic simulations in drug design, *Med. Res. Rev.*, 2006, **26**(5), 1–29.
119 T. Chu, P. Tian, G. Wang, Y. Jia, S. Dai and C. Rong, *et al.*, An Atomically Dispersed Pd Sub-Metallene: Intermediate State of Single Atoms and Metal Bonds, *Adv. Mater.*, 2025, **37**(29), 1–10.
120 K. Deng, J. Yu, Q. Mao, R. Yang, H. Yu and Z. Wang, *et al.*, Superlattices in Ru Metallene Nanobelts for Robust Hydrogen Evolution Conflict of Interest, *Adv. Funct. Mater.*, 2025, **35**(23), 1–10.
121 C. Hu, Q. Ma, S. F. Hung, Z. Chen, D. Ou and B. Ren, *et al.*, In Situ Electrochemical Production of Ultrathin Nickel Nanosheets for Hydrogen Evolution Electrocatalysis, *Chem*, 2017, **3**(1), 1–27.
122 G. Feng, P. Li and Y. Bi, Single-Crystalline Ultrathin Nickel Nanosheets Array from In Situ Topotactic Reduction for Active and Stable Electrocatalysis, *Angew. Chem., Int. Ed.*, 2015, **55**(2), 693–697.
123 B. Liu and N. Zhang, Cobalt-based nanosheet arrays as efficient electrocatalysts for overall water splitting, *J. Mater. Chem. A*, 2017, **33**, 1–5.
124 H. Weiju, Y. Dongxue, X. Qiuyu, W. Ruirui, Z. Chenglong, G. Yanhui, S. Ruimin, H. Mingxian and Z. Chen, Highly Efficient Overall-Water Splitting Enabled via Grafting Boron-Inserted Fe-Ni Solid Solution Nanosheets onto Unconventional Skeleton, *Appl. Catal., B*, 2021, **292**(120188), 1–11.
125 H. Yu, J. Ke and Q. Shao, Two Dimensional Ir-Based Catalysts for Acidic OER, *Small*, 2023, **19**(48), 1–20.
126 J. Yang, Q. Shao, B. Huang, M. Sun and X. Huang, pH-Universal Water Splitting Catalyst: Ru-Ni Nanosheet Assemblies, *iScience*, 2019, **11**, 1–27.
127 Q. Yao, N. Zhang and M. Sun, Channel-Rich RuCu Nanosheets for pH-Universal Overall Water Splitting Electrocatalysis, *Angew. Chem., Int. Ed.*, 2019, **58**(39), 13983–13988.
128 G. Hai, X. Jia, K. Zhang, X. Liu, Z. Wu and G. Wang, High-performance oxygen evolution catalyst using two-dimensional ultrathin metal-organic frameworks nanosheets, *Nano Energy*, 2017, **2**(4), 1–24.
129 M. Zhao, T. Guo, W. Qian, Z. Wang, X. Zhao, L. Wen and D. He, Fe-incorporated Cobalt-based Metal-organic Framework Ultrathin Nanosheets for Electrocatalytic Oxygen Evolution, *Chemical*, 2021, **422**(37), 130055.
130 M. R. Kandel, U. N. Pan, D. R. Paudel, P. P. Dhakal, H. Kim and J. H. Lee, Composites Part B: Engineering Hybridized bimetallic phosphides of Ni – Mo, Co – Mo, and Co – Ni in a single ultrathin-3D- nanosheets for efficient HER and OER in alkaline media, *Composites, Part B*, 2022, **239**(109992), 1–10.
131 J. Lai and S. Guo, Design of Ultrathin Pt-Based Multimetallic Nanostructures for Efficient Oxygen Reduction Electrocatalysis, *Small*, 2017, **13**(48), 1–18.
132 J. Lai, F. Lin, Y. Tang, P. Zhou, Y. Chao and Y. Zhang, *et al.*, Efficient Bifunctional Polyalcohol Oxidation and Oxygen Reduction Electrocatalysts Enabled by Ultrathin PtPdM (M = Ni, Fe, Co) Nanosheets, *Adv. Energy Mater.*, 2019, **9**(8), 1–9.
133 W. Chen, W. Gao, P. Tu and T. Robert, Neighboring Pt Atom Sites in an Ultrathin FePt Nanosheet for the Efficient and Highly CO-Tolerant Oxygen Reduction Reaction, *Nano Lett.*, 2018, **18**(9), 5905–5912.
134 M. Ai, J. Sun, Z. Li, H. Liang and C. Liu, Mechanisms and Properties of Bismuthene and Graphene/Bismuthene Heterostructures as Anodes of Lithium-/Sodium-Ion Batteries by First-Principles Study, *J. Phys. Chem. C*, 2021, **125**(21), 11391–11401.
135 J. Pan, Y. Sun, P. Deng, F. Yang, S. Chen, Q. Zhou, H. S. Park, H. Liu and B. Y. Xia, Hierarchical and ultrathin copper nanosheets synthesized via galvanic replacement for selective electrocatalytic carbon dioxide conversion to carbon, *Appl. Catal., B*, 2019, **255**, 25517736.
136 Y. Zhao, X. Tan, W. Yang, C. Jia, X. Chen and W. Ren, Surface Reconstruction of Ultrathin Palladium Nanosheets during, *Angew. Chem., Int. Ed.*, 2020, **59**(48), 21493–21498.
137 M. Wang, H. Shi, M. Tian, R. Chen, J. Shu, Q. Zhang, Y. Wang, C. Li, N. Wan and S. Lei, Single Nickel Atom-Modified Phosphorene Nanosheets for Electrocatalytic CO2 Reduction, *ACS Appl. Nano Mater.*, 2021, **4**(10), 1–8.
138 Y. Xu and H. Cao, Liquid-Phase Exfoliation of Graphene: An Overview on Phase Exfoliation Media, Techniques, and Challenges, *Nanomaterials*, 2018, **8**(11), 1–78.
139 X. Guo, X. Wan and J. Shui, Molybdenum-based materials for electrocatalytic nitrogen reduction reaction, *Cell Rep. Phys. Sci.*, 2021, **2**(6), 1–51.
140 J. Y. Ji, W. Zhang, C. Li, Y. Cao, J. Xue, H. Gu and J. P. Lang, In Situ Fe/Co/B Codoped MoS 2 Ultrathin Nanosheets Enable Efficient Electrocatalytic Nitrogen Reduction, *ACS Appl. Mater. Interfaces*, 2024, **16**(32), 41734–41742.

141 Y. Li, C. Cheng, S. Han, Y. Huang, X. Du, B. Zhang and Y. Yu, Electrocatalytic Reduction of Low-Concentration Nitric Oxide into Ammonia over Ru Nanosheets, *ACS Energy Lett.*, 2022, **7**(3), 1–10.

142 Z. H. Yuan, B. Sun, W. Zhong, X. Ai, J. Z. Gao, L. G. Feng and Y. Chen, Architecture Engineering and Phase Engineering of Rhodium Metallene Co- Boost Nitrite-to-Ammonia Electroconversion, *Angew. Chem.*, 2025, **64**(40), 1–10.

143 Y. Zhou, L. Zhang and M. Wang, Maximized atom utilization in a high-entropy metallene via single atom alloying for boosted nitrate electroreduction to ammonia, *Nat. Commun.*, 2025, **7915**, 1–36.

144 S. Bulletin, Vertically-interlaced NiFeP/MXene electrocatalyst with tunable electronic structure for high-efficiency oxygen evolution reaction, *Sci. Bull.*, 2021, **66**(11), 1063–1072.

145 Y. Liu, J. Zhang, T. Yan, G. Jin, J. Zhao, Y. Wang, X. Peng, H. Ma, J. Xu and D. Wang, High-performance Ru metallene cathode via 2D MXenes interface tailoring in Li-CO 2 batteries, *Energy Storage Mater.*, 2025, **76**(104144), 1–7.

146 H. Huang, D. Xiao, Z. Zhu, C. Zhang, L. Yang and H. He, *et al.*, A 2D/2D heterojunction of ultrathin Pd nanosheet/MXene towards highly efficient methanol oxidation reaction: the significance of 2D material nanoarchitectonics, *Chem. Sci.*, 2023, **36**, 1–19.

147 J. Cherusseri, S. A. Thomas and D. N. Rajendran, Ultrathin 2D metallenes for energy storage: a myth or reality?, *RSC Sustain.*, 2025, **9**, 1–35.

148 T. Ramachandran, L. Zheng and H. Butt, Energy nexus: MXene – MOF – chalcogenide hybrids triboelectric nanogenerators (TENGs) for self- powered supercapacitor storage with machine learning insights, *Mater. Today Adv.*, 2026, **29**, 2–4.

149 C. Wang, S. Liu, Y. Yamauchi, F. B. Zhang and Y. V. Kaneti, Ultrathin nanosheet-assembled nickel-based metal–organic framework microflowers for supercapacitor applications, *Chem. Commun.*, 2022, **7**, 1–5.

150 Y. Wang, H. Wang, Y. Liu, Y. Li, J. Zhang and H. Hou, *et al.*, Ultrathin NiCo-MOF Nanosheets for High-Performance Supercapacitor Electrodes, *ACS Appl. Energy Mater.*, 2019, **2**(58), 1–9.

151 X. Zhong, X. Liu, Z. Li, C. Wang and S. Dmytro, Electrodeposited ultra-thin FeCo 2 O 4 nanosheets on nickel foam as binder-free electrodes for high-performance supercapacitors, *J. Energy Storage*, 2023, **79**(109257), 1–8.

152 W. Qinfang, Z. Yunhe, Y. Jing, S. Dalei, C. Rongrong, L. Qi and L. Rumin, Controlled growth of hierarchical FeCo2O4 ultrathin nanosheets and Co3O4 nanowires on nickle foam for supercapacitors, *Int. J. Hydrogen Energy*, 2019, **44**(60), 1–8.

153 Y. Wang, Y. Liu, C. Wang, H. Liu, J. Zhang, J. Lin, J. Fan, T. Ding, J. E. Ryu and Z. Guo, Significantly Enhanced Ultrathin NiCo-based MOF Nanosheet Electrodes Hybrided with Ti 3 C 2 Tx MXene for High Performance, *Eng. Sci.*, 2020, **9**, 50–59.

154 J. Yang, C. Yu, C. Hu, M. Wang, S. Li and H. Huang, *et al.*, Surface-Confined Fabrication of Ultrathin Nickel Cobalt-Layered Double Hydroxide Nanosheets for High-Performance Supercapacitors, *Adv. Funct. Mater.*, 2018, **28**(44), 1–11.

155 K. Nasrin, V. Sudharshan, K. Subramani and M. Sathish, Insights into 2D/2D MXene Heterostructures for Improved Synergy in Structure toward Next-Generation Supercapacitors: A Review, *Adv. Funct. Mater.*, 2022, **32**(18), 1–6.

156 D. K. Sharma, S. Kumar, A. Laref and S. Auluck, Mono and bi-layer germanene as prospective anode material for Li-ion batteries: A first-principles study, *Comput. Mater. Sci.*, 2018, **69**, 1–9.

157 C. Tang, S. Wang, K. Zhang and C. Cheng, Remarkable-cycling-performance anode for Li-ion battery: The bilayer β -bismuthene, *Electrochim. Acta*, 2021, **388**(138641), 1–8.

158 J. Su, X. Wang, T. Duan, W. Li, B. Xiao and G. Zhou, *et al.*, A first-principles study of 2D antimonene electrodes for Li ion storage, *Appl. Surf. Sci.*, 2018, **462**, 270–275.

159 W. Tian, S. Zhang, C. Huo, D. Zhu, Q. Li and L. Wang, Few-Layer Antimonene: Anisotropic Expansion and Reversible Crystalline-Phase Evolution Enable Large-Capacity and Long-Life Na-Ion Batteries, *ACS Nano*, 2018, **12**(2), 1887–1893.

160 T. Ramachandran, From lab to market: the future of zinc – air batteries powered by MOF/MXene hybrids, *J. Mater. Chem. A*, 2025, **13**, 12855–12890.

161 S. A. Shubham, Electrochemical properties of stanene as an efficient anode material for Na-ion batteries, *Comput. Condens. Matter.*, 2021, **14**, 84–89.

162 L. Wu, P. Lu, R. Quhe, Q. Wang, C. Yang and P. Guan, *et al.*, Stanene nanomeshes as anode materials for Na-ion batteries, *J. Mater. Chem. A*, 2018, **17**, 1–5.

163 B. Mortazavi, A. Dianat, G. Cuniberti and T. Rabczuk, Application of silicene, germanene and stanene for Na or Li ion storage: A theoretical investigation, *Electrochim. Acta*, 2016, **213**, 865–870.

164 P. Panigrahi, Y. Pal, T. Hussain and R. Ahuja, Application of germanene monolayers as efficient anchoring material to immobilize lithium polysulfides in Li-S batteries, *Appl. Surf. Sci.*, 2021, **558**(149850), 1–8.

165 M. I. Khan, M. Khurshid, S. S. Alarfaji and A. Majid, Bismuthene as a novel anode material of magnesium/zinc ion batteries with high capacity and stability: a DFT calculation, *Phys. Chem. Chem. Phys.*, 2024, **42**, 21–25.

166 R. Khan, R. Mohan, N. Kalla, T. Ramachandran, P. Somu and J. Lee, *et al.*, Transition metal dichalcogenides for next-generation supercapacitors: Recent advances, challenges, and future perspectives, *J. Alloys Compd.*, 2025, **1039**, 1–7.

167 T. Ramachandran, R. Mohan, N. Kalla, Y. A. Kumar and A. Ghosh, Al- AG, *et al.* Black phosphorus as a multifunctional electrode material for all energy storage devices, *J. Alloys Compd.*, 2025, **1037**, 1–7.

168 E. Aspects, Beyond traditional MXenes: The promise of non-Ti MXenes in energy and catalysis, *Colloids Surf., A*, 2025, **726**, 1–6.

169 Z. Bo, Z. Zheng, Y. Huang, P. Chen, J. Yan and K. Cen, Covalently bonded MXene @ Antimonene heterostructure anode for fast lithium-ion storage, *Chem. Eng. J.*, 2024, **485**(149837), 1–8.